AD_____

Award Number: DAMD17-03-1-0407

TITLE: Mullerian Inhibiting Substances (MIS) Augments IFN-γ Mediated Inhibition of Breast Cancer Cell Growth"

PRINCIPLE INVESTIGATOR: Vandana Gupta, Ph.D.

CONTRACTING ORGANIZATION: Massachusetts General Hospital
                                                     Boston, MA 02114-2696

REPORT DATE: June 2006

TYPE OF REPORT: Annual Summary

PREPARED FOR: U.S. Army Medical Research and Materiel Command
                            Fort Detrick, Maryland 21702-5012

DISTRIBUTION STATEMENT: Approved for Public Release;
                                           Distribution Unlimited

The views, opinions and/or findings contained in this report are those of the author(s) and should not be construed as an official Department of the Army position, policy or decision unless so designated by other documentation.

REPORT DOCUMENTATION PAGE		*Form Approved* *OMB No. 0704-0188*

Public reporting burden for this collection of information is estimated to average 1 hour per response, including the time for reviewing instructions, searching existing data sources, gathering and maintaining the data needed, and completing and reviewing this collection of information. Send comments regarding this burden estimate or any other aspect of this collection of information, including suggestions for reducing this burden to Department of Defense, Washington Headquarters Services, Directorate for Information Operations and Reports (0704-0188), 1215 Jefferson Davis Highway, Suite 1204, Arlington, VA 22202-4302. Respondents should be aware that notwithstanding any other provision of law, no person shall be subject to any penalty for failing to comply with a collection of information if it does not display a currently valid OMB control number. **PLEASE DO NOT RETURN YOUR FORM TO THE ABOVE ADDRESS.**

1. REPORT DATE 01-06-2006	2. REPORT TYPE Annual Summary	3. DATES COVERED 1 Jun 2003 – 31 May 2006
4. TITLE AND SUBTITLE Mullerian Inhibiting Substances (MIS) Augments IFN-γ Mediated Inhibition of Breast Cancer Cell Growth"		**5a. CONTRACT NUMBER**
		5b. GRANT NUMBER DAMD17-03-1-0407
		5c. PROGRAM ELEMENT NUMBER
6. AUTHOR(S) Vandana Gupta, Ph.D.		**5d. PROJECT NUMBER**
		5e. TASK NUMBER
		5f. WORK UNIT NUMBER
7. PERFORMING ORGANIZATION NAME(S) AND ADDRESS(ES) Massachusetts General Hospital Boston, MA 02114-2696		**8. PERFORMING ORGANIZATION REPORT NUMBER**
9. SPONSORING / MONITORING AGENCY NAME(S) AND ADDRESS(ES) U.S. Army Medical Research and Materiel Command Fort Detrick, Maryland 21702-5012		**10. SPONSOR/MONITOR'S ACRONYM(S)**
		11. SPONSOR/MONITOR'S REPORT NUMBER(S)

12. DISTRIBUTION / AVAILABILITY STATEMENT
Approved for Public Release; Distribution Unlimited

13. SUPPLEMENTARY NOTES
 Original contains colored plates: ALL DTIC reproductions will be in black and white.

14. ABSTRACT

SEE ATTACHED PAGE

15. SUBJECT TERMS
Breast Cancer

16. SECURITY CLASSIFICATION OF:				18. NUMBER OF PAGES	19a. NAME OF RESPONSIBLE PERSON USAMRMC
a. REPORT U	**b. ABSTRACT** U	**c. THIS PAGE** U	UU	30	**19b. TELEPHONE NUMBER** *(include area code)*

Standard Form 298 (Rev. 8-98)
Prescribed by ANSI Std. Z39.18

ABSTRACT

MIS is a member of the TGFß family. The purpose of this study is to test the hypothesis that MIS and IFN-g might be moreeffective in the inhibition of breast cancer cell growth than either agent alone. We observed MIS and IFN-g co-stimulate IRF1 expressionthrough NFkB and STAT pathways, respectively with a synergistic induction of CEACAM1 and MHCII mRNA expression, genesdownstream of IRF1. In concordance with this observation, treatment of MDA-MB-468 cells with either MIS or IFN-g inhibited growth andthe presence of both inhibited growth better. We observed that MIS promotes IFN-g-induced apoptosis demonstrating a functionalinteraction between these two classes of signaling molecules in regulation of breast cancer cell growth. To evaluate whether MIS and IFN-gmay be useful in breast cancer therapy, we determined whether the growth inhibitory effect of MIS and IFN-g observed in vitro would berecapitulated in vivo. Both MIS and IFN-g decreased the gain in tumor volume of MDAMB468 xenografts established in SCID mice.C3(1)Tag transgenic mouse model carries the SV40 large T antigen targeted to the epithelium of the mammary and prostate glands andprogression of disease in these animals correlates well with progressive stages of human breast cancer. Mammary tumors arising in theC3(1) T antigen mouse model expressed the MIS type II receptor. Administration of MIS to mice was associated with a lower number ofpalpable mammary tumors and the mean mammary tumor weight as compared with the control group (p=0.029). Different doses of mIFN-gwere injected into 10 week old C3(1)Tag transgenic mice for 5 weeks intraperitoneally. Both 10ng and 100ng mIFN-g significantly reducedthe tumor volumes and tumor weights in this mouse model. Analysis of PCNA expression and caspase-3 cleavage in tumors revealed thatexposure to MIS or mIFN-g was associated with decreased proliferation and increased apoptosis, respectively, and not due to decline in T-antigen expression. Thus MIS and mIFN-g can suppress the growth of mammary tumors in vivo. Since, MIS improves the growth inhibitoryeffects of mIFN-g on breast cancer cell lines in vitro by augmenting IFN-gamma induced gene expression and apoptosis. Next, we treatedC3SV40 transgenic mice with mIFN-g(10ng) and MIS (20ug) independently and in combination for 4 weeks. We observed that micereceiving both MIS and mIFN-g had less mean tumor volume as compared to mice receiving independent treatments. Thus, these resultsdemonstrate that MIS can improve the growth inhibitory effects of IFN-gamma in vivo. This study indicates the possibility of using MIS.

Table of Contents

Introduction

Mullerian Inhibiting Substance (MIS) is a member of the TGFß family, a class of molecules that govern a myriad of cellular processes including growth, differentiation, and apoptosis. However, a postnatal role for MIS in males and females has yet to be defined. MIS inhibits breast cancer cell growth by interfering with cell cycle progression and inducing apoptosis. We recently demonstrated the presence of MIS receptors in mammary tissue and in breast cancer cell lines suggesting that the mammary gland is a likely target for MIS (Segev, et al, 2000). In the rat mammary gland, expression of the MIS type II receptor is suppressed during puberty when the ductal system branches and invades the adipose stroma and during massive expansion at pregnancy and lactation, but is upregulated during involution, a time of tissue regressio. The decline in MIS type II receptor expression during various stages of postnatal mammary growth suggested a growth suppressive role for MIS in the mammary gland (Segev et al, 2001).

Interferon regulatory factor-1 (IRF-1), a gene known for its growth inhibitory functions in breast cancer cells is induced by MIS and IFN-γ through a NFkB and STAT pathway respectively. Treatment of breast cancer cells with MIS and interferon-γ (IFN-γ) co-stimulated the expression of IRF-1 and CEACAM1, a target gene of IRF1. A combination of IFN-γ and MIS inhibited the growth of breast cancer cells to a greater extent than either one alone as assessed by MTT assay. Both reagents significantly decreased the fraction of cells in the S-phase of the cell cycle, an effect not enhanced when they were used in combination. Thus the enhanced inhibition of breast cancer cell growth by MIS and IFN-γ could not be explained by combined changes in cell cycle progression compared to treatment with either agent alone (Hoshiya et al, 2003).

We have demonstrated that MIS promotes IFN-γ-induced apoptosis demonstrating a functional interaction between these two classes of signaling molecules in regulation of breast cancer cell growth. To evaluate whether MIS and IFN-γ may be useful in breast cancer therapy, we determined whether the growth inhibitory effect of MIS and IFN-γ observed *in vitro* would be recapitulated *in vivo*. Assaying the effect of MIS on mammary tumor models *in vivo* is critical to determine whether MIS could act as an anti-tumor agent. We have developed human breast cancer xenografts in SCID mice using MDA-MB-468 cells and demonstrated that both MIS and IFN-γ-when injected intraperitoneally can inhibit the growth of these breast cancer xenografts in mice. Using a C3(1)Tag mouse model, which carries the SV40 large T antigen targeted to the epithelium of the mammary and prostate glands and develops spontaneous mammary tumors, we have observed that mean mammary tumor weight and growth of tumors in IFN-γ and MIS treated animals to be significantly lower than the vehicle treated controls. Analysis of PCNA expression and caspase-3 cleavage in tumors revealed that exposure to MIS was associated with decreased proliferation and increased apoptosis, respectively.

Since, MIS improves the growth inhibitory effects of IFN-γ on breast cancer cell lines in vitro by augmenting IFN-gamma induced gene expression and apoptosis. Next, we treated C3SV40 transgenic mice with mIFN-γ(10ng) and MIS (20ug) independently and in combination for 4 weeks. We observed that mice receiving both MIS and mIFN-γ had less mean tumor volume as compared to mice receiving independent treatments. Thus, these results demonstrate that MIS can improve the growth inhibitory effects of IFN-gamma in vivo. This study indicates the possibility of using MIS independently or in combination with IFN-gamma as an alternative therapy for the breast cancer cure.

4

Final Report (Body)

Title: Mullerian Inhibiting Substance (MIS) augments IFN-γ mediated inhibition of breast cancer cell growth.

Specific Aim I: Characterization of the molecular mechanism that integrates IFN-γ and MIS mediated signaling. (12 months)

Task 1: To identify the molecular mechanism by which MIS and IFN-γ induce IRF-1 expression in breast cancer cells. (completed)

MIS and IFN-γ function through distinct molecular pathways.

MIS and IFN-γ induce IRF-1 expression in breast cancer cells. In order to identify the molecular mechanisms, by which MIS and IFN-γ induce IRF-1 expression, gel shift assays were carried out using NFkB or STAT-inducing element (SIE) oligonucleotides containing the relevant DNA binding consensus sequences. MIS induced NFkB DNA binding activity. The supershift experiments performed using anti p50 and anti p65 antibodies demonstrated that the complex consists of p50 and p65 NFkB subunits in T47D cells (figure 1a). Binding to the SIE DNA sequence was not observed suggesting that MIS does not evoke STAT DNA binding in these cells. IFN-γ however induced SIE DNA binding activity but did not activate the DNA binding activity of NFkB. Antibody supershift experiments demonstrated that the STAT-DNA protein complex induced by IFN-γ contained the STAT-1 protein but not STAT-3 or STAT-5a (figure 1b).
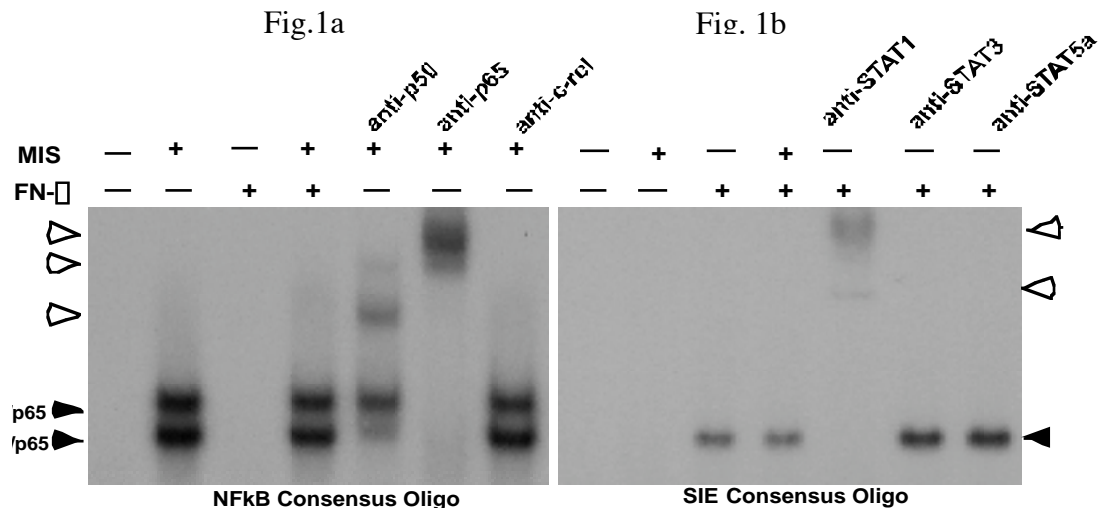

Fig. 1. T47D cells were treated with 35 nM MIS or 1 ng/ml of IFN-γ or both for 1 hour and 3 μg of nuclear proteins were analyzed by gelshift assay using 32P-labelled oligonucleotides containing the consensus DNA binding site for NFkB (a) or the STAT (b) proteins. (SIE: Stat Inducing Element)

MIS and IFN-γ costimulate IRF1 expression through NFkB and STAT pathway.

T47D cell clones, which express the dominant negative inhibitor of IkB (IkBα-DN) were generated. Induction of IRF-1 by MIS was greatly reduced in the clone harboring IkBα-DN compared to cells transfected with the empty vector, however it did not interfere with induction of IRF-1 by IFN-γ. MIS and IFNg costimulated the IRF1 expression in T47D cells via NFkB and STAT pathway (fig. 2) (JBC, 2003).
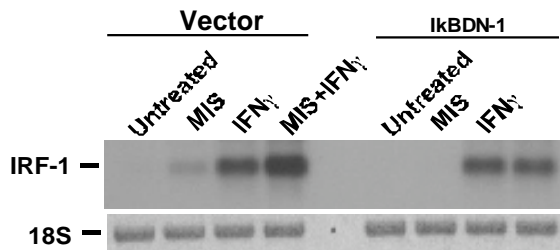

Fig. 2. Vector and IκBα-DN-expressing T47D cells were treated with 35 nM MIS or 1 ng/ml of IFN-γ or both for 2 hours and total RNA (5µg) was analyzed for IRF-1 expression.

Task 2: To determine if MIS mediated activation of IRF-1 occurs via Smad pathway (completed).

Induction of IRF1 by MIS is independent of the Smad pathway

MIS a member of TGFb family signals through Smad1 pathway. T47D cells stably expressing the Smad1DN transgene gene in which serines at residues 462, 463 and 465 were converted to alanines were identified by northern blot. Similar levels of IRF-1 induction by MIS in vector and Smad1DN transfected T47D cells (fig. 3) demonstrated that MIS mediated induction of IRF-1 does not require phosphorylation of Smad1.
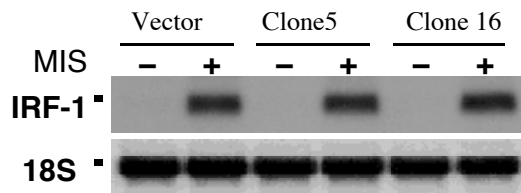

Fig. 3 Expression of IRF1 in vector transfected and Smad1DN was analysed by northern blot.

Task 3: To test the effect of MIS and IFN-γ on the gene expression of growth regulatory genes (completed)

MIS and IFN-γ induce the expression of CEACAM1 (JBC, 2003), p21 and MHC classII

CEACAM1 (carcinoembryonic antigen-realated cell adhesion molecule) also known as biliary glycoprotein (BGP) is a Ca^{2+} dependent cellular adhesion molecule that is expressed in epithelial cells (Thompson et al, 1994; Cheug et al, 1993). Both MIS and IFN-γ induced CEACAM1 expression in T47D cells. Interestingly, simultaneous addition of MIS and IFN-γ resulted in synergistic induction of CEACAM1 expression (figure 4a). IRF1 can inhibit tumor growth through the induction of p21, a growth inhibitory gene (Dornan et al, 2004). We observed that both MIS and IFN-γ induce p21 expression in T47D cells as observed by Western blot analysis but the expression was not further affected when cells were treated with a combination of MIS and IFN-γ for 4hrs (Fig. 4b)

MHC classII, another gene downstream of IRF1 was upregulated by IFN-γ (Storm

6

van's Gravesande, 2002). T47D cells when treated for 48hrs with MIS and IFN-γ demonstrated a synergistic induction of MHCII mRNA (Fig. 4c).

Thus, we have observed that MIS and IFN-γ costimulate the expression of IRF1 with a synergistic induction of the downstream genes CEACAM1 and MHCII in breast cancer cells.
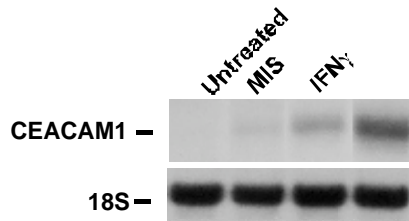
CEACAM1 —
18S —

Fig. 4a. T47D cells were treated with 35 nM MIS or 1 ng/ml of IFN-g or both for 24 hours. Total RNA isolated from cells was analyzed for CEACAM1 expression. Hybridization to 18S rRNA is shown.

	MIS		IFNg		MIS+ IFNg	
0	2	4	2	4	2	4

p21

Untreated MIS IFNg MIS+IFNg
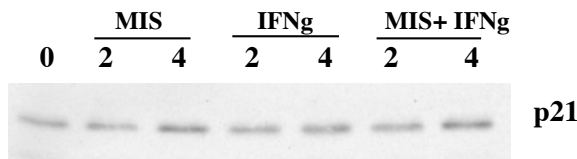
MHCII

Fig.4b. Expression of p21 in T47D cells treated with IFN-g(5ng/ml) and MIS (5ug/ml) for 2 and 4 hrs as assessed by Western blot analysis
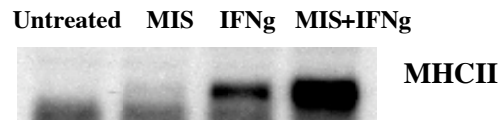
Fig.4c. Expression of MHCII in T47D cells treated with IFN-g(5ng/ml) and MIS (5ug/ml) for 48 hrs as assessed by Northern blot analysis

Specific Aim II: Test the effect of MIS, IFN-γ, or both on breast cancer cell growth using *in vitro* and *in vivo* model systems. (24 months)

Task 4: To characterize the mechanism by which MIS and IFN-γ inhibit breast cancer cell growth (completed)

Effect of MIS and IFN-γ on breast cancer cell growth

Since the signaling events initiated by MIS and IFN-γ converge to increase the magnitude of gene expression, we next tested their effect on the growth of breast cancer cells over a period of 1-8 days. Treatment of MDA-MB-468 cells with either MIS or IFN-γ inhibited growth and the presence of both inhibited growth better (figure 5; n=8).
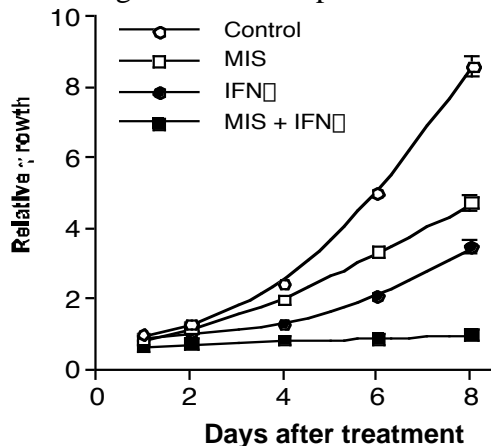
Fig. 5. MIS and IFN-g were added at a concentration of 35nM and 5ng/ml, respectively, to MDA-MB-468 cells seeded in a 96 well plate. Cell viability was determined after 1, 2, 4, 6 and 8 days by analysis of MTT conversion. Plates were anlyzed in an ELISA plate reader at 550 nm with a reference wave length of 630nm (n=8).

MIS and IFN-γ synergistically increased apoptosis (JBC, 2003, article attached).

Translocation of annexinV from the inner surface of the plasma membrane to the outside occurs after initiation of apoptosis and thus serves as a marker of apoptosis. MDA-MB-468 cells were treated with MIS, IFN-γ or MIS+IFN-γ for 96 hours and cell surface expression of annexinV was analyzed by staining cells with a FITC-annexinV antibody (Fig. 6a). Both MIS and IFN-γ increase number of annexin V positive cells. However, treatment of cells with a combination of MIS+IFN-γ together resulted in a synergistic increase in the fraction of cells in early and late stages of apoptosis. Thus growth inhibition of MDA-MB-468 cells following co-treatment with MIS and IFN-γ results from enhanced apoptosis.
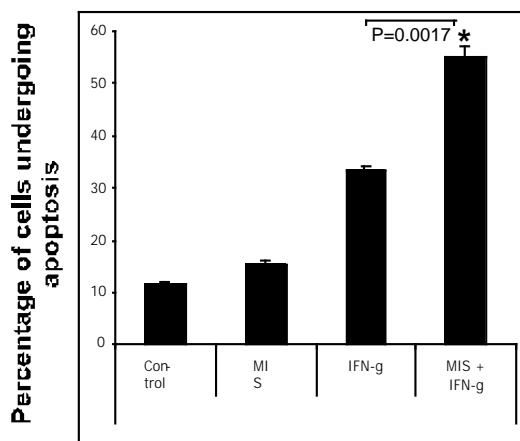

Early+ Late Stage apoptosis (Zones B+ C)

Fig. 6a MDA-MB-468 cells were treated with 5ng/ml IFNg or 5ug/ml MIS or both for 96 hrs. Cells were stained with annexinV-FITC and DAPI and analysed by FACS. Percentage of cells undergoing apoptosis is shown. Statistical analysis was done using ANOVA.

Thus, we have observed that a combination of MIS and IFN-γ led to a greater degree of growth inhibition compared with either agent alone due to enhanced apoptosis rather than a combinatorial effect on cell cycle progression.

Effect of MIS and IFN-γ on activated caspase-3

Both MIS and IFN-γ increased the cleaved caspase3, an apoptosis marker in MDA-MB-468 cells with an increase in the activated/ cleaved caspase3 when cells were treated in combination with MIS and IFN-γ for 3 days as demonstrated by Western blot analysis in fig. 6b
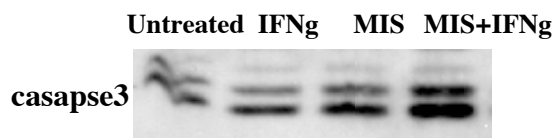

Untreated IFNg   MIS MIS+IFNg

casapse3

Fig. 6b MDAMB468 cells were treated with MIS(5ug/ml) and IFN-γ(5ng/ml) for 3 days. Activated caspase3 was assessed using Western blot analysis.

Task 5: To test the growth inhibitory effect of MIS and IFN-γ in vivo, selection of mouse model (completed).

In order to test the effect of MIS and IFN-γ *in vivo*, we tested MDA-MB-468 and T47D breast cancer cell lines in nude and SCID mice by injecting the cells subcutaneously on the dorsal flanks. MDA-MB-468 breast cancer cell line formed xenografts robustly in SCID mice.

Establish xenografts in SCID mice

The MDA-MB-468 cells are ER negative, Rb negative, harbor a mutant p53 and are highly responsive to MIS and rhuIFN-γ treatment *in vitro*.

$4x10^6$ cells/site in 50µl of DMEM were injected subcutaneously into the bilateral dorsal flanks of, 6-week old female SCID mice. Tumors appeared within one week of injections and did not demonstrate central necrosis. Mice were ear-tagged to monitor the kinetics of tumor growth at each site. Four weeks after the injection of cells, animals with tumors > 250mm^3 were randomly divided into treatment groups. Thus, the SCID animals with MDA-MB-468 xenografts established on the dorsal flanks were used for further studies.

Spontaneously arising mammary tumors in mice

A transgenic mouse model for spontaneous mammary carcinoma was obtained from Dr. Jeffrey Green at NIH, in which targeted expression of the early region of the SV40 large tumor Ag was achieved using the promoter of the rat prostatic steroid binding protein. Mammary tumors in this model occur in 100% of mice with very early onset. Atypia of the mammary gland develops at ~8 weeks progressing to intraepithelial neoplasia resembling human DCIS at ~12 weeks with development of invasive carcinomas at about ~16-24 weeks. It has also been utilized in several studies to test novel therapeutic strategies on various stages of tumor progression (Wigginton , 2001). These tumors are ER negative and have functionally inactive p53 and Rb and thus complement MDA-MB-468 xenografts in SCID mice (Yin et al, 2001).

Task 6: Determining the dose of MIS and IFN-γ required for tumor regression studies *(completed)*.

Female SCID mice were injected with a single dose of 1µg rhuIFN-γ and blood samples were drawn at various time intervals. Serum rhuIFN-γ concentrations, estimated based on a standard concentration curve, increased in proportion to the dose, peaked at ~1-3 hours and was undetectable at 24 hours. Serum of animals injected with 10 and 100 ng rhuIFN-γ once intraperitoneally had undetectable levels of rhuIFN-γ 6-24 hrs after injection. Although, rhuIFN-γ as high as 10µg injected once intraperitoneally did not cause any harmful effects to the animals but because of the known toxic effects of IFN-γ, 10-100ng rhuIFN-γ will be injected intraperitoneally to these animals 5 days a week for 4-5 weeks

Human and mouse interferon-γ proteins share 41% sequence homology and are species specific. Thus mouse IFN-γ (mIFN-γ; R & D systems) will be used to inject C3SV40 Tantigen mouse.

Previously, we have observed that 10μg rhMIS/ animal inhibits the growth of human ovarian cancer cell xenografts grown in nude mice (Drs. Patricia Donahoe and David McLaughlin; personal communication). Since, this dose had no harmful effects on animals and in order to further improve its anti-tumor effects we have injected 20 μg rhMIS/ animal intraperitoneally for 5 days a week with two treatment free days/ for 4-5 weeks.

Task 7: Once optimal dosages are estimated, animals with established tumors will be divided into four groups to administer (1) vehicle, (2) MIS, (3) IFN-γ and (4) MIS + IFN-γ. Serum MIS and IFN-γ concentration will be measured by ELISA. The tumor size will be measured by using calipers (completed).

Ia) Effect of MIS on MDA-MB-468 tumor growth in SCID mice

Results published in Gupta et al, PNAS 2005 (article attached)

I b) MIS inhibits the growth of spontaneously arising mammary tumors in C3(1) Tag mice *in vivo*

Results published in Gupta et al, PNAS 2005 (article attached)

IIa) Effect of IFN-γ on MDA-MB-468 tumor growth in SCID mice

MBA-MB-468 xenografts were grown subcutaneously and bilaterally in the dorsal flanks of 6-week old female SCID mice. A set of 10 mice with established tumors were divided into two groups of 5 each. Both groups were treated at the same time with either PBS or 10ng rhu IFN-γ/animal for 5 days a week with a treatment free interval of two days for 4 weeks. Volume was calculated as LxW^2 [length=L and width=W] at regular intervals. Gain in volume was calculated at the end of the treatment. IFN-γ significantly reduced the growth of xenografts as compared to control animals (p=0.0043).
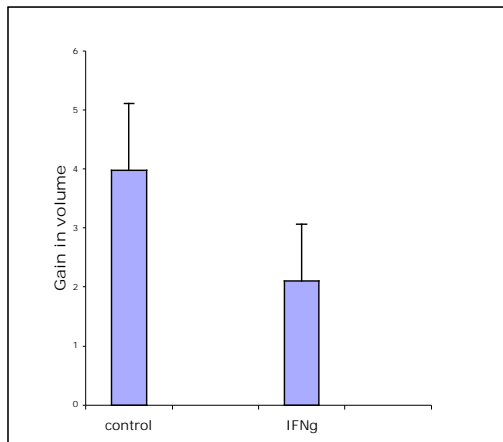

Fig.7. Effect of IFN-γ on MDA-MB-468 tumor xenografts established in SCID mice. Tumor volumes were measured during treatment using calipers.

IIb) IFN-γ inhibits the growth of cells established from C3(1) Tag mice

10

In order to test the effect of low levels of IFN-γ on mammary tumor growth *in vivo*, we first determined if IFNγ could inhibit the *in vitro* growth of M6 cells established from C3(1) Tag mouse tumors. M6 cells (2500/ well) were treated with 0, 10, and 100 ng/ml of IFN-γ for 6 days and cells numbers were quantified at 4, 5 and 6 days of treatment. As shown in figure 8, both 10 and 100ng/ ml mIFN-γ inhibited the growth of M6 cells by 51%, 74% and 86%, respectively (p<0.001 by two-sided Students' t-test) suggesting that these mammary tumor cells are responsive to the growth inhibitory effects of IFNγ.
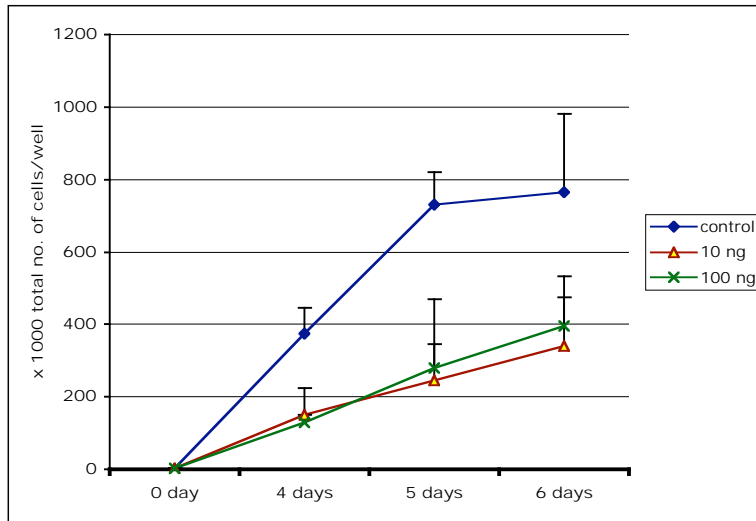

Fig.8. M6 cells were treated with different concentrations of mIFN-γ. Number of cells were counted over a period of 6 days after the treatment.

Effect of IFN-γ on the growth of mammary tumors in C3(1)SV40Tantigen animals

C3(1)SV40Tantigen transgenic mice were divided into three groups of 8 mice each. 10-week old mice were injected with 1) PBS 2) 10ng mIFN-γ   3) 100 ng mIFN-γ each day for 5 days a week for 5 weeks. Two weeks after the start of treament animals started having palpable tumors which were measured at regular intervals using calipers. At the end of the experiment, animals were sacrificed and tumors excised and weighed. Mice receiving mIFN-γ had significantly less number of tumors as compared to control animals (Fig. 9) and the tumor growth in these mice was very slow compared to PBS animals in which tumors once appeared grew robustly. However, some of the mIFN-γ treated groups with no palpable tumors also had hyperplasia or early stages of tumorigenesis. Animals receiving 10ng mIFN-γ had a 50% decrease in tumor weight (p=0.03) with a 70% decrease (p=0.009) in mice receiving 100ng mIFN-γ as compared to PBS receiving mice after 5 weeks of treatment (Fig. 9b).
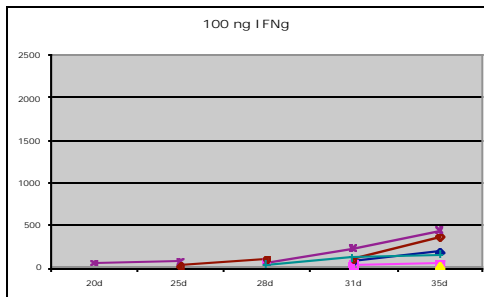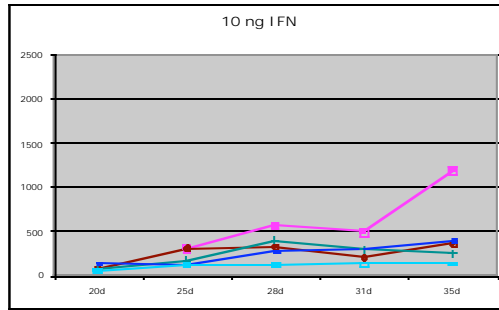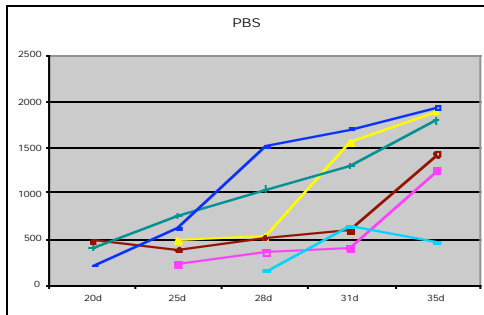
Fig. 9. C3 SV40Tag mice divided into three groups received PBS or 10 or 100ng mIFN-g 5 weeks. Tumor volumes were measured at regular intervals using callipers.
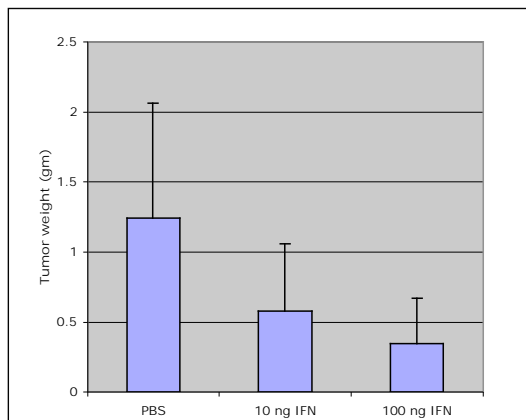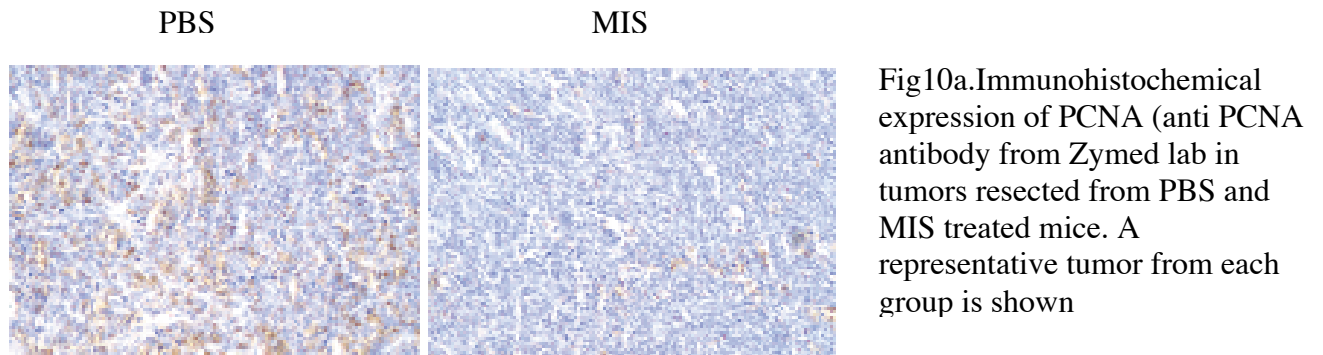

Fig.9b Effect of mIFN-γ on the mean tumor weights in C3SV40 after 5 weeks of treatment.

Task 8: The tumors will be tested histopathologically to evaluate the histology of grafts (completed).

Both MIS and IFN-γ suppress proliferation of mammary tumors *in vivo*

In order to determine whether suppression/delay in mammary tumors observed in MIS and IFN-γ treated mice was due to decreased proliferation and/or increased apoptosis compared with that observed in PBS-treated controls, tumors were stained with antibodies against PCNA, a marker of proliferation, and cleaved caspase-3, a marker of early stage apoptosis. The extent of PCNA staining in the mammary adenocarcinomas resected from PBS-treated animals was uniform through out the tumors while the MIS-treated adenocarcinomas demonstrated PCNA positive regions interspersed with PCNA negative patches (figure 10 a). The nodular atypical hyperplasia and mammary

12

intraepithelial neoplasia in the mammary glands of MIS-treated mice also demonstrated patchy PCNA staining.

PBS   MIS

Fig10a.Immunohistochemical expression of PCNA (anti PCNA antibody from Zymed lab in tumors resected from PBS and MIS treated mice. A representative tumor from each group is shown

In case of tumors from Interferon gamma treated mice, PCNA staining was dramatically decreased in both 10ng and 100ng IFN gamma treated animals.

PBS   10ng IFNg   100ng IFNg
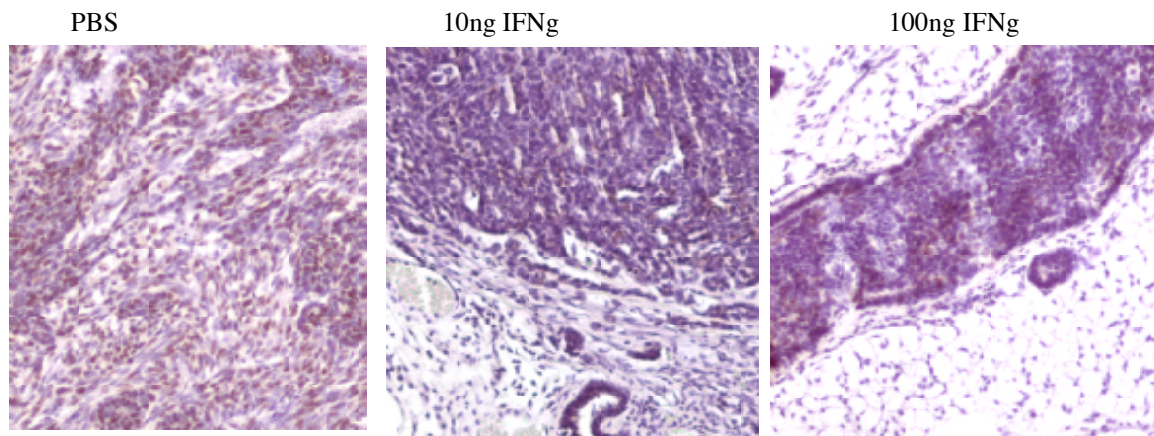

Fig. 10b.Immunohistochemical expression of PCNA in tumors resected from PBS and Interferon gamma treated mice. A representative tumor from each group is shown

Activated caspase3 was increased in MIS treated tumors as compared to PBS. In IFNgamma treated animals also staining for cleaved caspase3 was prominent and most of the tumors from Interferon gamma treated mouse stained positive for cleaved caspase3 as assessed by Immunohistochemistry analysis of tumors from PBS and Interferon gamma treated mice.
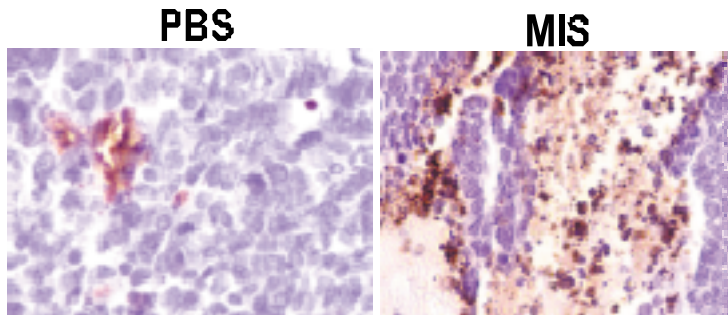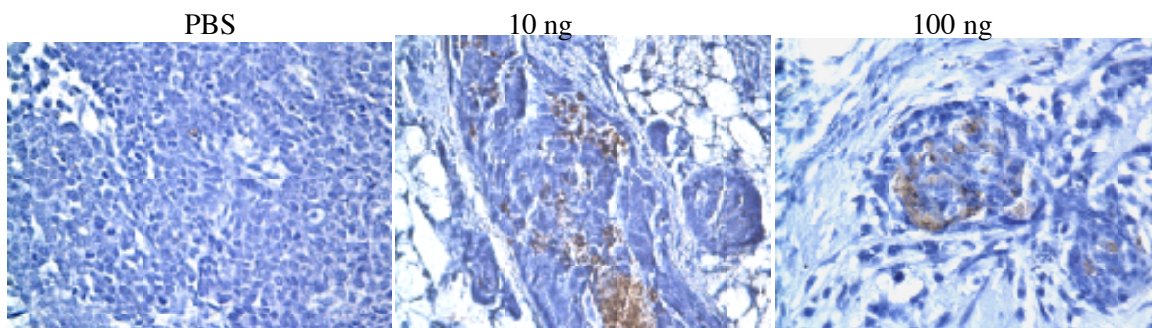
Fig. 11 a

Fig. 11b

Fig. 11a, b. Caspase3 cleavage in PBS and MIS treated tumors (Fig. 11a) and PBS and IFN-γ treated tumors (Fig. 11b) as assessed by immunohistochemically using anti caspase3 antibody from Cell Signalling. A representative tumor from each group is shown

III) To test if MIS and IFN-γ can inhibit the breast tumor growth better than MIS or IFN-γ alone *in vivo*

10 week old mice were divided into four groups of 5 animals each and received 1) PBS; 2) mIFN-γ (10ng/ day); 3) MIS (20ug/ day); 4) MIS (20ug) + mIFN-γ (10ng)/ day for 5 days a week with a treatment free interval of 2 days for a total of 4 weeks. Two weeks after the start of treatment animals start showing palpable tumors. Tumor volumes were measured at regular intervals during the treatment and tumor weights were measured at the end of treatment. Tumor volumes which were obtained by LxWxW were found to be decreased in all the groups as compared to PBS control. Both MIS and mIFN-γ reduced the tumors weights independently, however the combined treatment of MIS and mIFN-γ reduced both the tumor weights and tumor volumes further as compared to the independent treatments. Thus, these results suggest that MIS can improve the growth inhibitory effects of IFN-γ (fig. 12).
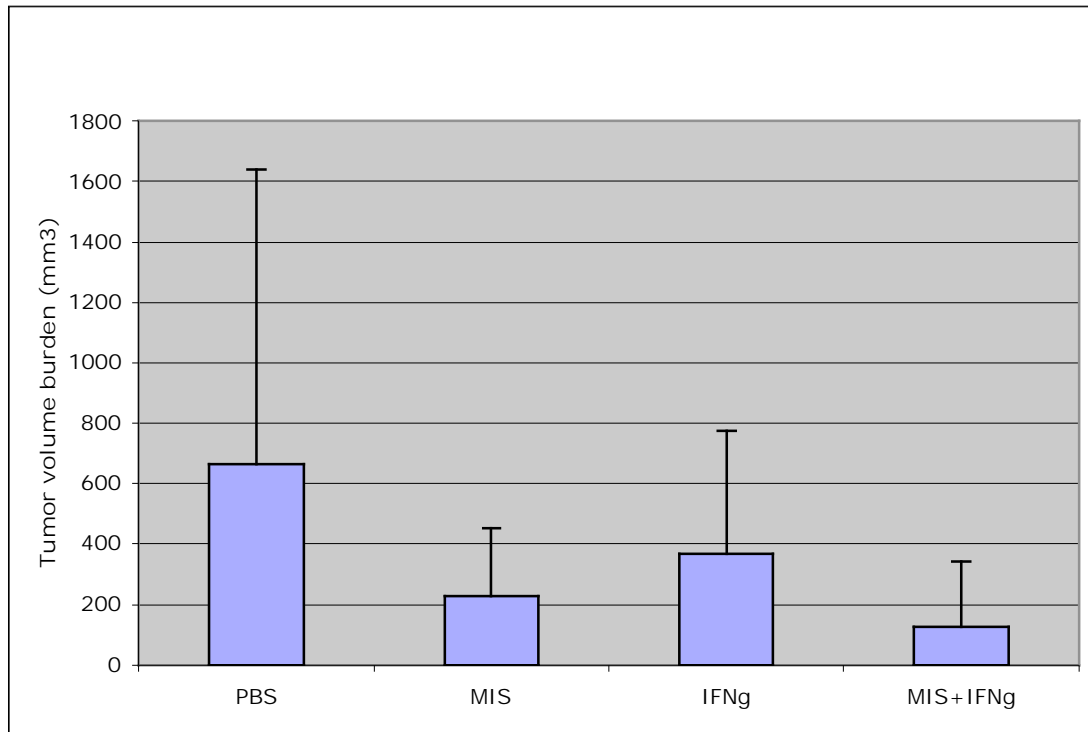
14

Fig. 12. C3Sv40 mice were divided into four groups of 5 mice each and received PBS, 10ng mIFNg, 20ug MIS independently or in combination for 4 weeks and the tumor volumes were measured as LxWxW.

Key Accomplishments:

MIS and IFN-γ function through distinct molecular pathways. MIS induced NFkB DNA binding activity in breast cancer cells where as IFN-γ functions through Stat1 DNA binding activity as is observed by Gel shift assays.

MIS and IFN-γ costimulate IRF1 expression in breast cancer cells through activation of NFkB and STAT pathways, respectively.

MIS mediated induction of IRF-1 does not require phosphorylation of Smad1 as similar levels of IRF-1 induction are observed by MIS in vector and Smad1DN transfected T47D cells.

MIS and IFN-γ costimulate the expression of IRF1 with a synergistic induction of the downstream genes CEACAM1 and MHCII in breast cancer cells.

Treatment of MDA-MB-468 cells with either MIS or IFN-γ inhibited growth and the presence of both inhibited growth better.

MIS and IFN-γ co-stimulate the expression of activated caspase3, an apoptosis marker in MDA-MB-468 cells.

MIS and IFN-γ together resulted in a synergistic increase in the fraction of cells in early and late stages of apoptosis as observed by enhanced translocation of annexinV from the inner surface of the plasma membrane to the outside, which occurs after initiation of apoptosis.

To test the growth inhibitory effect of MIS and IFN-γ *in vivo,* MDA-MB-468 xenografts were established by bilaterally injecting $4x10^6$ cells/site in 50μl of DMEM subcutaneously onto the dorsal flanks of SCID mice.

For *in vivo* experiments, IFN-γ and MIS doses are determined. 10- 100ng rhuIFN-γ were injected intraperitoneally to the SCID animals and mIFN-γ to C3SV40Tantigen mice, 5 days a week with two treatment free days/ for 4 weeks.

MIS treatment (20 ug/ animal for 5 days a week with two treatment free days/ for 4 weeks) decreased the rate of mean volume gain of tumors established as xenografts in SCID mice as compared to vehicle treated group.

Administration of MIS to C(3)SV40Tantigen mice with spontaneous mammary tumors was associated with a lower number of palpable mammary tumors compared with vehicle-treated mice, and the mean mammary tumor weight in the MIS-treated group was significantly lower compared with the control group.

rhuIFN-γ (10ng) reduced the net gain in tumor volumes as well as tumor weights of the MDAMB468 xenografts in SCID mice.

Adiministration of mIFN-γ (10ng or 100ng) per day for 5 days a week for 5 weeks to C3SV40Tag mice resulted in a decrease in net tumor weight and tumor volume in these mice.

Analysis of PCNA expression and caspase-3 cleavage in tumors revealed that exposure to MIS as well as IFN-γ was associated with decreased proliferation and increased apoptosis, respectively, and not due to decline in T-antigen expression.

In order to test if combined administration of MIS and IFN-γ can improve the growth inhibitory effects of IFN-γ, we injected 20ug MIS,10ng mIFN-γ or a combination of MIS and IFN-γ to C3SV40Tag mice for 4 weeks and tumor weights and volumes were measured. Mice receiving both MIS and IFN-γ had less mean tumor weights and voulumes as compared to either treatment alone. Thus these results suggest that MIS may improve the growth inhibitory effects of IFN-γ and possibly we can further reduce the dose of IFN-γ in combination with MIS as MIS does not have any known toxic effects.

Reportable outcomes:

Publications:
1. **V. Gupta**, Carey JL, Kawakubo H, Muzikansky A, Green JE, Donahoe PK, Maclaughlin DT, Maheswaran S. Mullerian inhibiting substance suppresses tumor growth in the C3(1)T antigen transgenic mouse mammary carcinoma model. **Proc. Natl. Acad. Sci USA**, 2005, 102: 3219-3224.

2. **V. Gupta**, D. P. Harkin, H. Kawakubo and S. Maheswaran. Transforming growth factor-β superfamily: Evaluation as breast cancer biomarkers and preventive agents. Current Cancer Drug Targets, 2004, 4, 1-11.

3. Y. Hoshiya, **V. Gupta**, H. Kawakubo, E. Brachtel, J.L.Carey, L.M.Sasur, A. Scott, P.K. Donahoe and S. Maheswaran. Mullerian inhibiting substance promotes

interferon γ induced gene expression and apoptosis in breast cancer cells. The Journal of Biological Chemistry, 2003, 278, 51703-12.

Presentations:

1. **Gupta V**, Carey JL, Kawakubo H, Muzikansky A, Green JE, Donahoe PK, Maclaughlin DT, Maheswaran S. Mullerian inhibiting substance suppresses tumor growth in the C3(1)T antigen transgenic mouse mammary carcinoma model. Era of Hope, June 8- 11, 2005, Philadelphia Convention Center, Philadelphia.

2. "MIS promotes interferon-γ mediated apoptosis of breast cancer cells".
   V. Gupta, Y. Hoshiya and S. Maheswaran at "Molecular Targets of Breast and Prostate Cancer" 2003 Joint retreat for Programs of Cell Biology, Breast cancer and Prostate cancer in the DF/ HCC.

3. **"**MIS promotes IFN-γ-induced gene expression and apoptosis in breast cancer cells. **Vandana Gupta**, Yasunori Hoshiya, Hirofumi Kawakubo, Elena Brachtel, Jennifer L. Carey, Laura Sasur, Andrew Scott, Patricia K. Donahoe and Shyamala Maheswaran at the SAC Poster 2003, MGH.

4. " Mullerian Inhibiting Substance promotes interferon induced IRF-1 expression and suppression of breast cancer cell growth" **V. Gupta**, Y. Hoshiya, P.K.Donahoe and S. Maheswaran at AACR, Feb. 2004 at Orlando, FL.

Conclusions:

1. MIS and IFN-γ function through distinct molecular pathways in breast cancer cells.
2. MIS and IFN-γ induce IRF1 expression in T47D cells through NFkB and STAT pathway repectively.
3. MIS mediated induction of IRF1 expression does not require Smad1 phosphorylation.
4. MIS and IFN-γ synergistically induce CEACAM1 and MHC11 expression in T47D cells.
5. MIS improves the growth inhibitory effect of IFN-γ in breast cancer cells.
6. MIS and IFN-γ together resulted in a synergistic increase in the fraction of cells undergoing apoptosis.
7. MDA-MB-468 cells grow robustly as xenografts in SCID mice when injected as $4x10^6$ cells/site in 50μl of DMEM subcutaneously onto the dorsal flanks.
8. MIS treatment decreased the rate of mean volume gain of tumors established as xenografts in SCID mice as compared to vehicle treated group.
9. Administration of MIS to C(3)SV40Tantigen mice with spontaneous mammary tumors was associated with a lower number of palpable mammary tumors and the mean mammary tumor weight as compared with the control group.
10. Interferon gamma reduced the growth of MDA-MB-468 xenografts in SCID mice.

11. Both 10ng and 100ng mIFNgamma reduced the growth of tumors and net tumor weight of mammary tumors in C3SV40Tag mice.
12. Analysis of PCNA expression and caspase-3 cleavage in tumors revealed that exposure to either MIS or IFN-γ was associated with decreased proliferation and increased apoptosis, respectively, and not due to decline in T-antigen expression.
13. To test if MIS and IFN-γ can reduce the growth of mammary tumors better than IFN-γ alone, mice with spontaneously arising tumors (C3SV40Tag) received both MIS (20ug) and IFN-γ (10ng) in combination or independently for 4 weeks. At the end of treatment mice receiving combination of MIS and IFN-γ had lesser tumor weights and volumes as compared to either MIS or IFN-γ treated mice.

References:

1. Segev, D. L., Ha, T. U., Tran, T. T., Kenneally, M., Harkin, P., Jung, M., MacLaughlin, D. T., Donahoe, P. K. & Maheswaran, S. (2000) *J Biol Chem* 275, 28371-9.
2. Segev, D. L., Hoshiya, Y., Stephen, A. E., Hoshiya, M., Tran, T. T., MacLaughlin, D. T., Donahoe, P. K. & Maheswaran, S. (2001) *J Biol Chem* 276, 26799-806.
3. Hoshiya, Y., Gupta, V., Kawakubo, H., Brachtel, E., Carey, J. L., Sasur, L., Scott, A., Donahoe, P. K. & Maheswaran, S. (2003) *J Biol Chem* **278,** 51703-12.
4. Dornan D, Eckert M, Wallace M, Shimizu H, Ramsay E, Hupp TR, Ball KL. Mol Cell Biol. 2004; 24(22):10083-98.
5. Storm van's Gravesande K, Layne MD, Ye Q, Le L, Baron RM, Perrella MA, Santambrogio L, Silverman ES, Riese RJ. (2002) J Immunol.;168(9):4488-94.
6. Cheung, P. H., Thompson, N. L., Earley, K., Culic, O., Hixson, D., and Lin, S. H. (1993) *J Biol Chem* 268, 6139-6146
7. Thompson, N. L., Lin, S. H., Panzica, M. A., and Hixson, D. C. (1994) *Pathobiology* 62, 209-220.
8. Wigginton, J. M., Park, J. W., Gruys, M. E., Young, H. A., Jorcyk, C. L., Back, T. C., Brunda, M. J., Strieter, R. M., Ward, J., Green, J. E., and Wiltrout, R. H. (2001) *J Immunol* **166**, 1156-1168.
9. Yin, F., Giuliano, A. E., Law, R. E. & Van Herle, A. J. (2001) *Anticancer Res* **21,** 413-20.
10. Gupta, V., Carey, J.C., Kawakubo, H., Green, J., Donahoe., P.K. and Maheswaran, S. (2005) PNAS, 102, 3219-3224.

Appendix

Mullerian inhibiting substance suppresses tumor growth in the C3(1)T antigen transgenic mouse mammary carcinoma model

V. Gupta*[†], J. L. Carey*[†], H. Kawakubo*[†], A. Muzikansky[‡], J. E. Green[§], P. K. Donahoe[†¶], D. T. MacLaughlin[†¶], and S. Maheswaran*[†‖]

Departments of *Surgical Oncology and ‡Biostatistics, and ¶Pediatric Surgical Research Laboratories, Massachusetts General Hospital, and †Harvard Medical School, Boston, MA 02114; and §Laboratory of Cell Regulation and Carcinogenesis, National Institutes of Health, Bethesda, MD 20892

Mullerian inhibiting substance (MIS) inhibits breast cancer cell growth *in vitro*. To extend the use of MIS to treat breast cancer, it is essential to test the responsiveness of mammary tumor growth to MIS *in vivo*. Mammary tumors arising in the C3(1) T antigen mouse model expressed the MIS type II receptor, and MIS *in vitro* inhibited the growth of cells derived from tumors. Administration of MIS to mice was associated with a lower number of palpable mammary tumors compared with vehicle-treated mice ($P = 0.048$), and the mean mammary tumor weight in the MIS-treated group was significantly lower compared with the control group ($P = 0.029$). Analysis of proliferating cell nuclear antigen (PCNA) expression and caspase-3 cleavage in tumors revealed that exposure to MIS was associated with decreased proliferation and increased apoptosis, respectively, and was not caused by a decline in T antigen expression. The effect of MIS on tumor growth was also evaluated on xenografted human breast cancer cell line MDA-MB-468, which is estrogen receptor- and retinoblastoma-negative and expresses mutant p53, and thus complements the C3(1)Tag mouse mammary tumors that do not express estrogen receptor and have functional inactivation of retinoblastoma and p53. In agreement with results observed in the transgenic mice, MIS decreased the rate of MDA-MB-468 tumor growth and the gain in mean tumor volume in severe combined immunodeficient mice compared with vehicle-treated controls ($P = 0.004$). These results suggest that MIS can suppress the growth of mammary tumors *in vivo*.

proliferation | apoptosis | simian virus 40 large T antigen

Mullerian inhibiting substance (MIS) is a member of the TGF-β family, a class of molecules that govern a myriad of cellular processes including growth, differentiation, and apoptosis. Synthesis of MIS demonstrates a sexually dimorphic pattern and is produced by Sertoli cells of the fetal and adult testis and granulosa cells of the postnatal ovary. In male embryos, MIS causes regression of the Mullerian duct, the anlagen of the Fallopian tubes, uterus, and upper vagina (1). However, a postnatal role for MIS in males and females has yet to be defined. Signaling by MIS is propagated by binding of MIS to the MIS type II receptor, a transmembrane serine, threonine kinase expressed at high levels in the Mullerian duct, Sertoli cells, and granulosa cells of the embryonic and adult gonads and in the uterus (2–4). The MIS-bound type II receptor subsequently recruits a type I receptor. Activin-like kinase 2 (ALK2), ALK3, and ALK6 have been implicated in mediating MIS signaling in cells (5–9).

We recently demonstrated the presence of MIS receptors in mammary tissue and breast cancer cell lines, suggesting that the mammary gland is a likely target for MIS (6, 10, 11). In the rat mammary gland, expression of the MIS type II receptor is suppressed during puberty when the ductal system branches and invades the adipose stroma and during massive expansion at pregnancy and lactation, but is up-regulated during involution, a time of tissue regression (11, 12). The decline in MIS type II receptor expression during various stages of postnatal mammary growth suggested a growth-suppressive role for MIS in the mammary gland. Consistent with this concept, MIS inhibited the growth of both estrogen receptor-positive and -negative breast cancer cells by inducing cell cycle arrest and apoptosis (10). Moreover, injection of MIS into female mice induced apoptosis in the epithelium of mammary tissue compared with vehicle-injected control animals (11).

To evaluate whether MIS may be useful in breast cancer therapy, we determined whether the growth inhibitory effect of MIS observed *in vitro* would be recapitulated *in vivo*. Assaying the effect of MIS on mammary tumor models *in vivo* is critical for determining whether MIS could act as an antitumor agent in a milieu replete with several growth factors that promote tumor growth. The C3(1)Tag transgenic mouse model carries the simian virus 40 (SV40) large T antigen targeted to the epithelium of the mammary and prostate glands. The transgenic female mice spontaneously develop atypical ductal hyperplasia by 8 weeks, nodular atypical hyperplasia by 12 weeks, and invasive carcinomas by 16–20 weeks. Disease progression in this model occurs within a relatively short period and correlates well with progressive stages of human breast cancer (13), and has been used in several studies to test novel therapeutic strategies on various stages of mammary tumor progression (13, 14).

The oncogenic SV40 large T antigen-induced tumorigenesis involves functional inactivation of the tumor suppressor genes retinoblastoma (*Rb*) and *p53* (15, 16), and invasive carcinomas arising in this model are estrogen-independent. Mutations in *Rb* are prevalent in 20% of human breast cancers and *p53* mutations/alterations are detected in ≈50% of primary human breast tumors (17, 18), suggesting that inactivation of these two tumor suppressors may be critical in human breast tumorigenesis. The estrogen receptor-negative human breast cancer cell line MDA-MB-468 is *Rb* negative, harbors mutant *p53*, overexpresses the *EGF* receptor (19), and is highly responsive to MIS treatment *in vitro* (20). Thus testing the efficacy of MIS in severe combined immunodeficient (SCID) mice bearing MDA-MB-468 tumors would validate the antitumor studies in the C3(1)Tag model for spontaneous mammary carcinoma. In this study, we evaluated whether MIS can inhibit the growth of mammary tumors in the C3(1)Tag model as well as MDA-MB-468 xenografts established in SCID mice. Our results demonstrate that MIS suppresses the growth of mammary tumors *in vivo* in both experimental systems.

Methods

Cell Lines, Reagents, and Growth Inhibition Assays. The M6 tumor cells established from C3(1)Tag mice and MDA-MB-468 cells

APPLIED BIOLOGICAL SCIENCES

were grown in DMEM supplemented with 10% female FBS, glutamine, and penicillin/streptomycin. To measure inhibition of M6 cell proliferation by MIS, cells were plated in a 24-well plate at a density of 2,500 cells per well and treated with 1, 5, and 10 μg/ml of MIS for 4 days. Cell numbers were quantified by using a hemocytometer. Recombinant human MIS was immunoaffinity-purified from CHO cells transfected with the human MIS gene (21) followed by desalting and concentration by centricon (Millipore) and quantification by the BioRad method.

Antibodies and Western Blot Analyses. The rabbit MIS type II receptor antibody has been described (22). The anti-SV40 large Tag antibody was purchased from Pharmingen, and the anti-cleaved caspase-3 antibody was from Cell Signaling Technology, Beverly, MA. Western analysis was performed as described (23).

Animal Studies. *C3(1)Tag Mice.* All animals were cared for and experiments were performed at The Wellman Animal Facility, Massachusetts General Hospital under American Association for Laboratory Animal Science guidelines using protocols approved by the Institutional Review Board-Institutional Animal Care and Use Committee of the Massachusetts General Hospital. A pair of young homozygous male and female C3(1)Tag mice were used to build a mouse colony. Twenty-five 10-week-old female mice (consisting of seven separate litters born 2–3 days apart) were randomized into two groups to receive PBS (vehicle control, 13 animals) and 20 μg of MIS per animal per day (12 animals) by i.p. injections. Animals were injected for 5 days with 2 days of treatment-free interval for 6 weeks. Mice were monitored daily for evidence of toxicity and found to be healthy and active during the entire course of treatment. None of the animals had externally visible tumors at the commencement of treatment. Three weeks after treatment began palpable tumors emerged in some animals. At the end of the experiment, animals were killed, and tumors were excised, weighed, and snap-frozen or fixed for histologic and biochemical evaluation.

MIS ELISA (24) to determine MIS concentration in blood collected from mice at the end of the experiment was analyzed in duplicate at six serial dilutions by using a standard curve constructed with four-parameter logistical curve fitting Delta-Soft II (BioMetallics, Princeton, NJ). Assay sensitivity was 0.5 ng/ml; and the intraassay and interassay coefficients of variation were 9% and 15% respectively. The ELISA did not recognize luteinizing hormone, follicle-stimulating hormone, activin, inhibin, TGF-β, or bovine or rodent MIS.

SCID mice. MDA-MB-468 xenografts were established by bilaterally injecting 4×10^6 cells per site in 50 μl of DMEM s.c. into the dorsal flanks of 10 6-week-old female SCID mice maintained in the Edwin L. Steele Laboratory for Tumor Biology, Boston. Mice were ear-tagged to monitor the kinetics of tumor growth at each site. After ≈4 weeks palpable tumors were observed in 8 of 10 animals. Some developed tumors bilaterally (7/10), whereas another had just one tumor (1/10). The eight animals with palpable tumors were divided randomly into two treatment groups. The PBS-treated group had four animals, three of which had two tumors and one of which had one tumor. The MIS treatment group had four animals, each of which had two tumors.

Treatment of both groups began at the same time. The tumor volumes in the animals in the two groups were comparable. Mice were injected daily i.p. with PBS (100 μl) or 20 μg MIS per animal for 5 days a week with a treatment-free interval of 2 days. Tumors were measured by using calipers just before treatment began and at regular intervals throughout the treatment period. Volume was calculated as $L \times W^2$ (*L*, length; *W*, width). Serum MIS concentration was measured at the end of the experiment by MIS-ELISA.

Serum MIS Measurement. Blood was collected by cardiac puncture from PBS- and MIS-treated mice and placed in 1.5-ml microcentrifuge tubes to facilitate clot formation. The clots were centrifuged, and serum was removed to measure serum MIS concentrations as described (25).

Statistical Analyses. The number of measurable tumors in each group on the last day of treatment was compared by using one-sided Fisher's exact test. Differences were considered to be significant when $P < 0.05$.

The mean tumor weights at the end of the experiment in PBS- and MIS-treated C3(1)Tag mice were compared by using the Kruskal–Wallis test, and differences were considered to be significant when $P < 0.05$.

Because each mouse is an experimental unit our calculations are based on total tumor volume per animal. In MDA-MB-468 tumor-bearing SCID mice, tumor volumes were comparable between sites and were summed to obtain total tumor volume per animal. The gain in tumor volume per mouse, at the end of the experiment, was calculated as {tumor volume$_{Final}$ − tumor volume$_{Initial}$ ÷ tumor volume$_{Initial}$}. Statistical analysis was performed by using two-sided Student's t test. Differences were considered to be significant when $P < 0.05$.

Immunohistochemical Analyses. Tissues were fixed in formalin and embedded in paraffin. Sections of 5-μ thickness were stained with hematoxylin and eosin. To detect apoptosis, sections were immunostained with Cleaved Caspase-3 antibody (Asp-175, Cell Signaling Technology) according to the manufacturer's instructions. Briefly, sections were deparaffinized, treated with citrate buffer at subboiling temperature to retrieve antigen, and cooled, and peroxidase quench was added. The slides were washed and blocked, and primary antibody was added and incubated overnight. After washing three times, slides were incubated with secondary antibody for 30 min, and Avidin Biotin solution was added. Color was developed with substrate chromagen, and sections were counterstained with hematoxylin.

Proliferation in tumors was assessed by staining sections with the proliferating cell nuclear antigen (PCNA) staining kit (Zymed). Sections were treated with hydrogen peroxide to inhibit endogenous peroxidase, and antigen was retrieved by microwaving the samples in citrate buffer. Slides were stained with a biotinylated PCNA mAb (clone PC10) followed by streptavidin-peroxidase as a signal generator and diaminobenzidine as chromogen. Sections were counterstained with hematoxylin.

Results

MIS Inhibits the *in Vitro* Growth of Cells Established from Mammary Tumors Arising in C3(1)Tag Mice. We had demonstrated that MIS inhibits the growth of breast cancer cells *in vitro* (10). To confirm these observations *in vivo*, the effect of MIS on the growth of mammary tumors in the C3(1)Tag mice was tested. Western blot analysis of proteins isolated from mammary tumors in the C3(1)Tag mice demonstrated the expression of MIS type II receptor. Proteins extracted from vector and MIS type II receptor-transfected COS cells were used as negative and positive controls, respectively (Fig. 1*A*).

Before testing the effect of MIS on mammary tumor growth *in vivo*, we first determined whether MIS could inhibit the *in vitro* growth of M6 cells established from C3(1)Tag mouse tumors. M6 cells were treated with 1, 5, and 10 μg/ml of MIS for 4 days, and cell numbers were quantified. As shown in Fig. 1*B*, MIS inhibited the growth of M6 cells by 51%, 74%, and 86%, respectively ($P < 0.001$ by two-sided Student's t test), suggesting that these mammary tumor cells are responsive to the growth inhibitory effects of MIS. Consistent with this observation,
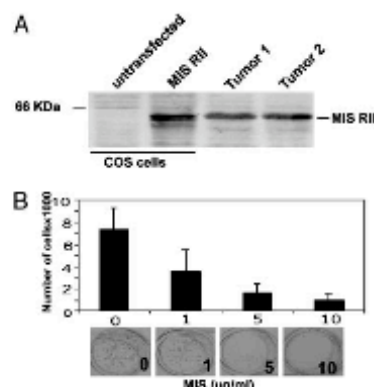
A

untransfected MIS RII Tumor 1 Tumor 2

66 KDa —   — MIS RII

COS cells

B

MIS (µg/ml)

Fig. 1. MIS inhibits M6 cell growth *in vitro*. (*A*) MIS type II receptor expression in C3(1)Tag mouse mammary tumors. Total protein from tumors was analyzed by Western blot. Untransfected and MIS type II receptor-transfected COS cells were used as negative and positive controls, respectively. Position of the MIS type II receptor protein is shown. (*B*) Equal numbers of M6 cells were treated with increasing concentrations of MIS. The number of cells in each well after 4 days of MIS treatment and a representative view of the wells is shown.

staining the cells for PCNA demonstrated that MIS suppressed the proliferation of M6 cells in culture (data not shown).

MIS Inhibits the Growth of Spontaneously Arising Mammary Tumors in C3(1)Tag Mice *in Vivo*. Two groups of 10-week-old mice were injected with either PBS or 20 µg of MIS daily for 5 days with 2 days of treatment-free interval for six cycles. The PBS- and the MIS-injected groups consisted of 13 and 12 mice, respectively. Externally palpable tumors were not observed in any of the animals at the commencement of treatment. One mouse in the MIS group was removed from the experiment within a week of treatment because of a large nonmammary tumor, which caused discomfort to the animal. Except for this animal, there was neither weight loss nor any other discernible adverse effects in the animals within the two groups.

During the course of treatment, 10 animals in the PBS-treated group and 6 animals in the MIS-injected group developed externally palpable tumors. Of the 10 animals that developed palpable tumors in the PBS-injected group, 7 presented with tumors on day 28, 1 on day 32, 1 on day 37, and another on day 42 of treatment. At death, an additional two animals in this group were found to have measurable tumors in their mammary gland. In the MIS-treated group, two animals presented with externally palpable tumors on day 28 of treatment, one presented on day 32, and an additional three animals presented with tumors on day 42. Interestingly the animals in this group, which did not present with externally palpable tumors, did not have any large tumor masses at death. These results indicate that by 42 days of treatment MIS exposure is associated with animals having fewer palpable tumors (Fig. 2*A*; *P* < 0.048 by one-sided Fisher's Exact test).

At the end of the experiment, animals were killed and tumors were excised and weighed. The tumor weights in the PBS-treated control animals ranged from 0.08 to 4.63 mg with a mean tumor weight of 0.71 mg and a median of 0.38 mg. The tumor weights in the MIS-treated animals ranged from 0.07 to 0.64 mg with a mean weight of 0.16 mg and a median of 0.10 mg. The lowest tumor (0.07 mg) in this group represents the total weight of micronodules of tumor that could not be excised free of normal tissue. The mean tumor weight in animals was significantly lower
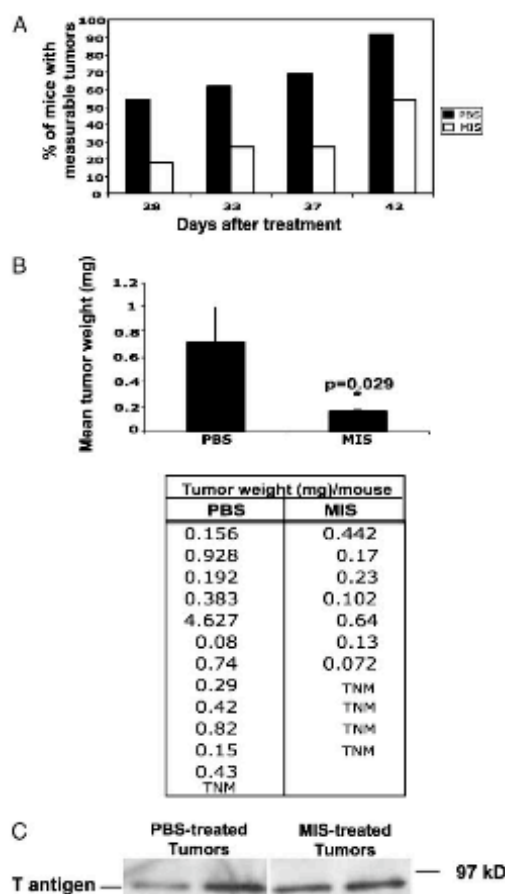

A

Days after treatment

B

Tumor weight (mg)/mouse	
PBS	**MIS**
0.156	0.442
0.928	0.17
0.192	0.23
0.383	0.102
4.627	0.64
0.08	0.13
0.74	0.072
0.29	TNM
0.42	TNM
0.82	TNM
0.15	TNM
0.43 TNM	

C

PBS-treated Tumors   MIS-treated Tumors

T antigen —   — 97 kD

Fig. 2. MIS treatment is associated with a decrease in the number of palpable tumors in animals. (*A*) Ten-week-old C3(1)Tag mice were injected with either PBS (*n* = 13) or MIS (*n* = 11), and animals were monitored for palpable tumors. The graph shows the percentage of animals with measurable tumors in each group vs. the days of treatment. On the 42nd day after treatment, the total number of measurable tumors was lower in the MIS group compared with the PBS group. *P* < 0.05 by one-sided Fisher's Exact test. (*B*) At the end of the experiment, animals were killed, and tumors were excised and weighed. The tumor weight in each animal is given. TNM (tumor not measurable) represents animals in which tumors could not be detected by palpation. The graph shows the mean tumor weight ± standard error in the PBS- and MIS-injected groups. (*C*) Proteins extracted from tumors in PBS- and MIS-treated animals were immunoblotted with an anti-SV40Tag antibody. The position of the SV40 large T antigen is shown.

in the MIS-treated group compared with controls (Fig. 2*B*; *P* = 0.029 by Kruskal–Wallis test). The statistical analysis was repeated excluding the largest tumor (4.627 mg) present in a mouse in the PBS-treated group and indicated that the difference in tumor weights between the two groups was still significant (*P* = 0.048). To ensure that the decrease in tumor growth in the MIS-treated animals was not caused by suppression of SV40 T antigen in tumors, tumor samples from PBS- and MIS-treated
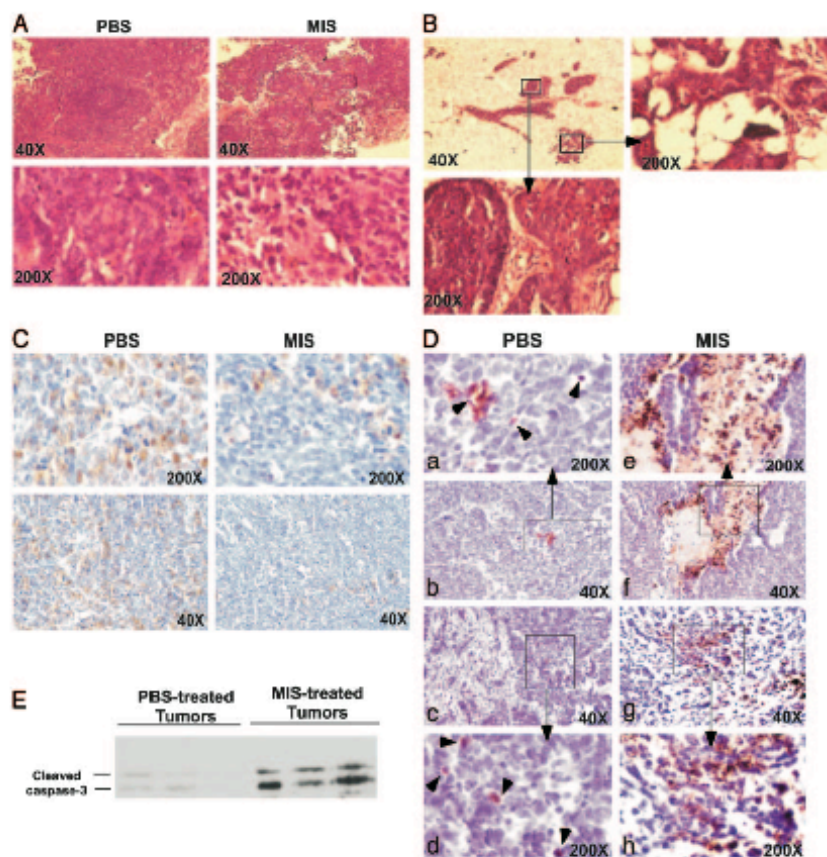
Fig. 3. MIS decreases proliferation and increases apoptosis in mammary tumors. (A) Hematoxylin and eosin staining of palpable mammary tumors excised from the MIS- and PBS-treated animals. Histology of a representative tumor is shown. (B) Histological analysis of the mammary glands of MIS-treated mice, which did not present with palpable tumors. The higher magnifications (*Insets*) demonstrate regions of atypical hyperplasia (*Right*) and mammary intraepithelial neoplasia (*Lower Left*). (C) PCNA expression in tumors resected from PBS- and MIS-treated mice. A representative tumor from each group is shown. (D) Caspase-3 cleavage in PBS- and MIS-treated tumors. (*b* and *c*) Tumors from two PBS-treated animals. (*a* and *d*) Higher magnifications of *b* and *c Insets* are shown in *a* and *d*, respectively. Arrowheads show cells positive for caspase-3 cleavage. (*f* and *g*) Tumors from two MIS-treated animals. (*e* and *h*) Higher magnifications of *f* and *g Insets* are shown in *e* and *h*, respectively. (*E*) Proteins extracted from PBS- and MIS-treated tumors were analyzed by Western blot using an antibody against cleaved caspase-3.

mice were analyzed by Western blot. As demonstrated in Fig. 2C, MIS treatment did not alter the expression of SV40 T antigen in tumors.

MIS Suppresses Proliferation and Induces Apoptosis in Mammary Tumors *in Vivo*. Both PBS- and MIS-treated animals with grossly palpable tumors had well developed invasive adenocarcinomas (Fig. 3A). Histological evaluation of tissues demonstrated that the mammary glands of MIS-treated animals that did not have externally palpable tumors had nodular atypical hyperplasia and mammary intraepithelial neoplasia, in which neoplastic cells filled the lumens of the duct, but did not present with invasive carcinomas (Fig. 3B). To determine whether suppression/delay in mammary tumors observed in MIS-treated mice was caused by decreased proliferation and/or increased apo-

ptosis compared with that observed in PBS-treated controls, tumors were stained with antibodies against PCNA, a marker of proliferation, and cleaved caspase-3, a marker of early-stage apoptosis. The extent of PCNA staining in the mammary adenocarcinomas resected from PBS-treated animals was uniform throughout the tumors, whereas the MIS-treated adenocarcinomas demonstrated PCNA-positive regions interspersed with PCNA-negative patches (Fig. 3C). The nodular atypical hyperplasia and mammary intraepithelial neoplasia in the mammary glands of MIS-treated mice also demonstrated patchy PCNA staining. These results indicate that mammary tumors exposed to MIS undergo less proliferation compared with those in PBS-treated controls.

Staining the tumors for activated caspase-3 revealed a marked increase in the number of apoptotic cells in the MIS-treated
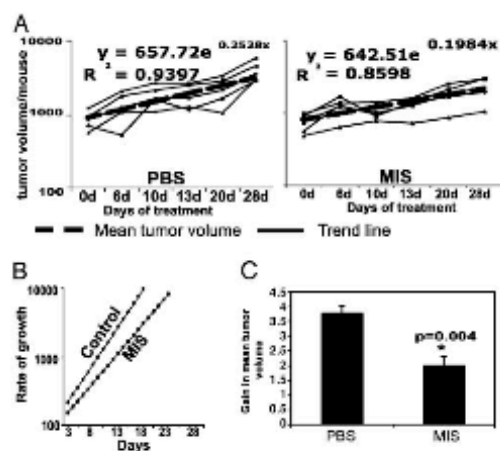
24

Fig. 4. MIS decreases the growth of MDA-MB-468 tumor xenografts established in SCID mice. (A) MDA-MB-468 tumor xenografts were established in mice. Animals with palpable tumors were treated with PBS ($n = 4$) or MIS ($n = 4$), and tumor volumes were measured. The graphs demonstrate changes in total tumor volume in each animal during the course of treatment in the two groups. The thick line represents the mean gain in tumor volume and the hatched line represents the trend line derived from the means, assuming that tumor growth is exponential. (B) The rates of tumor growth within the two groups were calculated based on the equations derived from trend lines. (C) The mean of the gain in tumor volume in each group ± standard error is shown; the gain in the MIS-treated group was significantly different from the PBS-treated group ($P < 0.005$ by two-sided Student's t test).

tumors compared with PBS-injected controls (Fig. 3D), suggesting that exposure to MIS induces apoptosis in the mammary tumors *in vivo*. This idea was also confirmed by immunoblotting tumor proteins for cleaved caspase-3 (Fig. 3E).

MIS Suppresses MDA-MB-468 Tumor Growth in SCID Mice. The human breast cancer cell line MDA-MB-468 is estrogen receptor-negative and *Rb*-negative and harbors mutant *p53*. MIS inhibits the growth of MDA-MB-468 cells *in vitro*. To validate and confirm the relevance of the results obtained in transgenic mice, we tested the growth inhibitory effects of MIS on MDA-MB-468 xenografts established in SCID mice. This experimental system closely complements the C3(1)Tag mouse mammary tumor model in which the tumors are estrogen-independent (13) and arise because of functional inactivation of Rb and p53 by the oncogenic T antigen (15, 16).

MDA-MB-468 xenografts were grown s.c. and bilaterally in the dorsal flanks of 6-week-old female SCID mice. After ~4 weeks, the eight animals with palpable tumors were randomized into two groups with four animals in the PBS control group and four mice in the MIS treatment group. Both groups were treated at the same time with either PBS or 20 μg MIS per animal for 5 days a week with a treatment-free interval of 2 days for 4 weeks. Volume was calculated as $L \times W^2$ (L, length; W, width) at regular intervals (Fig. 4A). Analysis of the rate of mean growth during the treatment demonstrated that tumors in the PBS group were growing more rapidly compared with tumors in the MIS-treated group (Fig. 4B). The gain in tumor volume over the course of treatment was calculated as volume at the end of treatment − volume at the beginning of treatment/volume at the beginning of treatment. The PBS group had a higher gain in tumor volume

than the MIS group (Fig. 4C; $P = 0.004$ by two-tailed Student's t test).

Discussion

The presence of MIS in the serum well after regression and differentiation of the Mullerian duct in males and females, respectively, (24, 26) suggests that MIS may have a postnatal role in adults. Moreover, the expression of MIS receptors in nongonadal tissues such as the mammary and prostate glands (10–12, 27) suggests additional functions for this hormone besides the induction of apoptotic regression of the Mullerian duct. We had demonstrated that MIS inhibits breast cancer cell growth *in vitro* by preventing cell cycle progression and inducing apoptosis (10). In this article, using two *in vivo* model systems, we demonstrate that administration of MIS suppresses mammary tumor growth in mice. We had previously injected a single dose of 100 μg of MIS into female mice and tested the induction of *IEX-1*, a MIS-inducible gene, in the mammary glands of mice. These results demonstrated that MIS at this high dose could induce the expression of *IEX-1* (11). Subsequently, Stephen *et al.* (28), tested the efficacy of MIS against ovarian cancer cell lines *in vivo* and reported that daily injections of 10 μg of purified exogenous recombinant human MIS suppressed tumor growth in immune-suppressed mice. Based on these results a comparable dose of MIS (20 μg per animal per day) was used in these experiments.

In the C3(1)Tag model, fewer animals in the MIS-treated group developed palpable tumors compared with PBS-injected controls. Although the measurable tumors in both groups progressed to adenocarcinomas, histological analyses of tumors indicated that tumors in the MIS-treated group were less dense compared with those in the PBS-treated group. This observation is consistent with the remarkable increase in apoptosis and curtailed proliferation in MIS-treated tumors compared with the PBS-injected controls. The presence of nodular atypical hyperplasia and mammary intraepithelial neoplasia in the MIS-treated mice that did not present with palpable tumors suggests that MIS may not block neoplastic transformation by the SV40 large tumor antigen but suppresses or delays tumor progression, resulting in the overall delay in the appearance of palpable tumors in the MIS-treated group.

This concept is further supported by the results observed in the MD-MB-468 xenograft model, in which administering MIS to animals with established tumors decreased the rate of tumor growth compared with vehicle-treated controls. Although the mean tumor weight at the end of the experiment was higher in the PBS group than in the MIS group (0.51 vs. 0.33 mg), this difference was not statistically significant ($P = 0.13$ by two-sided Student's t test). This finding was surprising given that the gain in mean tumor volume during the course of the experiment was significantly higher in the PBS-treated animals ($P < 0.004$) than in the MIS-treated mice. However, this result could reflect variations in initial tumor weights, which could not be measured.

The ability of MIS to inhibit MDA-MB-468 tumor growth in SCID mice is likely to occur directly at the cellular level because SCIDs harbor a mutation that severely impairs the development of T and B lymphocytes and MIS can inhibit MDA-MB-468 cell growth *in vitro*. Although MIS has no known immune modulatory effects, whether its inhibitory effect on mammary tumors arising in the immune-competent transgenic mouse model involves enhancement of host immune function remains to be determined. We recently demonstrated that MIS signaling intersects with the IFN-γ pathway and enhances IFN-γ induced expression of downstream target genes such as *IRF-1* and *CEACAM1*. Furthermore, a combination of MIS and IFN-γ led to a greater degree of growth inhibition of breast cancer cells compared with either agent alone because of enhanced apoptosis rather than a combinatorial effect on cell cycle progression (20). The C3(1)Tag mice would provide an excellent experimen-

Mullerian Inhibiting Substance Promotes Interferon γ-induced Gene Expression and Apoptosis in Breast Cancer Cells*

Yasunori Hoshiya, Vandana Gupta, Hirofumi Kawakubo, Elena Brachtel, Jennifer L. Carey,
Laura Sasur, Andrew Scott, Patricia K. Donahoe, and Shyamala Maheswaran‡

*From the Pediatric Surgical Research Laboratories, Massachusetts General Hospital and Harvard Medical School,
Boston, Massachusetts 02114*

This report demonstrates that in addition to interferons and cytokines, members of the TGFβ superfamily such as Mullerian inhibiting substance (MIS) and activin A also regulate IRF-1 expression. MIS induced IRF-1 expression in the mammary glands of mice *in vivo* and in breast cancer cells *in vitro* and stimulation of IRF-1 by MIS was dependent on activation of the NFκB pathway. In the rat mammary gland, IRF-1 expression gradually decreased during pregnancy and lactation but increased at involution. In breast cancer, the IRF-1 protein was absent in 13% of tumors tested compared with matched normal glands. Consistent with its growth suppressive activity, expression of IRF-1 in breast cancer cells induced apoptosis. Treatment of breast cancer cells with MIS and interferon γ (IFN-γ) co-stimulated IRF-1 and CEACAM1 expression and synergistic induction of CEACAM1 by a combination of MIS and IFN-γ was impaired by antisense IRF-1 expression. Furthermore, a combination of IFN-γ and MIS inhibited the growth of breast cancer cells to a greater extent than either one alone. Both reagents alone significantly decreased the fraction of cells in the S-phase of the cell cycle, an effect not enhanced when they were used in combination. However, MIS promoted IFN-γ-induced apoptosis demonstrating a functional interaction between these two classes of signaling molecules in regulation of breast cancer cell growth.

Mullerian Inhibiting Substance (MIS)[1] is a member of the TGFβ family, a class of molecules that regulates growth, differentiation, and apoptosis in many cell types. In the male embryo, MIS causes regression of the Mullerian duct, the an-

lagen of the Fallopian tubes, uterus, and the upper vagina (1). However, a postnatal role for MIS in males and females has yet to be clearly defined. MIS receptor mRNA in the mammary gland significantly diminishes during puberty when the ductal system branches and invades the adipose stroma and during the expansive growth at pregnancy and lactation, but is upregulated during involution, a time of regression and apoptosis (2, 3). The inverse correlation between MIS type II receptor expression and various stages of mammary growth suggests that MIS-mediated signaling may exert an inhibitory effect on mammary gland growth. Consistent with this concept, MIS inhibited the growth of both estrogen receptor (ER)-positive and -negative breast cancer cells by inducing cell cycle arrest and apoptosis (4).

Type I (IFN-α and IFN-β) and type II (IFN-γ) interferons are a family of antiviral cytokines that exhibit immunomodulatory and anti-proliferative effects (5). The antitumor effects of cytokines such as interleukin-12, in murine mammary carcinogenesis models correlate with high levels of serum IFN-γ (6–12). IFN-γ induced tumor regression results from immune surveillance of tumor cells and from direct cytotoxic effects (13–17), which are evident from its ability to inhibit the growth of several tumor-derived cell lines (18, 19) including breast cancer cells (20–22). Intralesional injections of IFN-α and IFN-γ into breast cancer patients with skin recurrences resulted in either complete or partial regression of the skin lesions but was associated with clinical toxicity in all patients (23). Thus identification of molecules that enhance the antitumor effects of IFN-γ may render it effective at lower doses, reduce clinical toxicity associated with high concentrations of the drug, and expand their therapeutic applications.

IFN-γ-induced growth inhibition requires coordinate expression of specific genes. Interferon regulatory factor-1 (IRF-1) is robustly induced by both type I and type II interferons. In addition to its important role in innate and adaptive immunity (24), IRF-1 also plays a role in regulating the growth of different mammalian cell lines (25). Different aspects of the tumor suppressor function of IRF-1 may be explained, at least in part, by the observation that it induces several growth regulatory genes including those with anti-proliferative activity such as IFNα/β, p21, and the cell adhesion molecule CEACAM1 (carcinoembryonic antigen-related cell adhesion molecule) (25).

Using DNA microarrays to profile gene expression, we identified that treatment of breast cancer cells with MIS strongly induces the expression of IRF-1. Since interferons also strongly induce IRF-1 (15), we tested whether intersection of MIS and
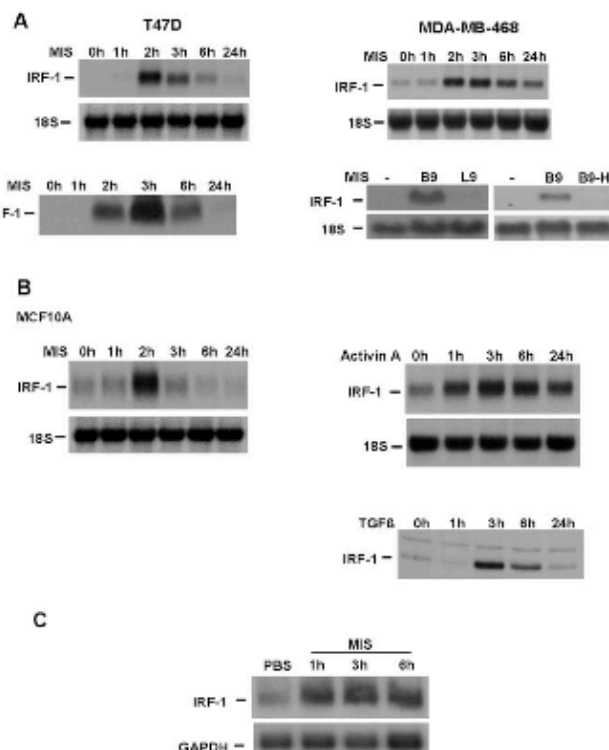
[1] The abbreviations used are: MIS, Mullerian inhibiting substance; IRF, interferon regulatory factor-1; IFN, interferon; MTT, 3-(4,5-dimethylthiazol-2-yl)-2,5-diphenyltetrazolium bromide; STAT, signal transducer and activator of transcription; FACS, fluorescence-activated cell sorter; DAPI, 4',6-diamidino-2-phenylindole; SIE, stat-inducing element; FITC, fluorescein isothiocyanate; CEACAM1, carcinoembryonic antigen-related cell adhesion molecule; EST, expressed sequence tag; PBS, phosphate-buffered saline; ELISA, enzyme-linked immunosorbent assay.

26

disease (30). Furthermore, both activin and TGFβ induced IRF-1 in MCF10A cells (Fig. 1*B, right panels*). Thus IRF-1 expression in mammary epithelial cells may be under the regulation of multiple members of the TGFβ family including MIS.

We next determined whether exposure of mammary glands to exogenous rhMIS would result in the induction of IRF-1 *in vivo.* Intraperitoneal injection of rhMIS into mice induced IRF-1 expression in the mammary glands compared with PBS-injected controls (Fig. 1*C*). The serum rhMIS levels averaged 2–4 μg/ml in the animals as measured by ELISA (26).

Expression of IRF-1 in the Rat Mammary Gland and in Human Breast Cancer—Expression analysis of IRF1 in the mammary glands of virgin, pregnant, lactating, and weaned rats demonstrated that IRF-1 mRNA was detectable in the virgin animals but gradually declined during pregnancy (G5-G21) and reached a nadir at late pregnancy (G17-G21) and lactation (PD0-PD10: lactating). Expression rebounded in the mammary glands of weaned rats (PD3-PD10: weaned) and reached the level observed in virgin animals 3 days after removal of pups (Fig. 2*A, upper* and *lower panels*).

Immunostaining with an anti-IRF-1 antibody demonstrated that IRF-1 was expressed predominantly in the epithelial cells of the ducts and lobules of the mammary gland. Expression pattern of the IRF-1 protein coincided with that of the IRF-1 mRNA; expression was detectable in the mammary glands of virgin and early pregnant (G5) animals but not during late pregnancy (G21) or in the lactating glands (Fig. 2*B, upper* and

lower panels). No signal was detected when sections were stained with either affinity-purified rabbit immunoglobulins or with anti-IRF-1 antibody preincubated with the cognate peptide (data not shown).

Since IRF-1 expression in the mammary epithelial cells decreased during pregnancy, a time at which the cells undergo massive proliferation, we wished to determine whether expression of the IRF-1 protein would be lower in breast tumor tissue compared with matched normal glands. We immunostained 23 tumors of various histologic grades with an anti-IRF-1 antibody. Expression of IRF-1 was absent in three tumors but present in the adjacent normal uninvolved ducts and lobules (Fig. 2*C, upper panel*). Two of these were of poorly differentiated histologic grade, and one tumor was moderately differentiated. In seven patients, staining for IRF-1 was patchy and limited to 20–80% of the tumor tissue (data not shown). In the other 13 patients expression of IRF-1 was detectable in both the tumor and the surrounding normal tissue (Fig. 2*C, lower panel*).

Since these results suggest a growth suppressive effect for IRF-1 in breast cancer, we analyzed whether IRF-1 could induce apoptosis of breast cancer cells. MDA-MB-468 cells in logarithmic growth phase were transiently transfected with a construct, which encodes for the IRF-1 protein, and a plasmid encoding the cell surface marker CD20 as described by Ref. 28. Vector-transfected cells were used as controls. Cells were fixed 72 h after transfection and stained for CD20 expression. An-
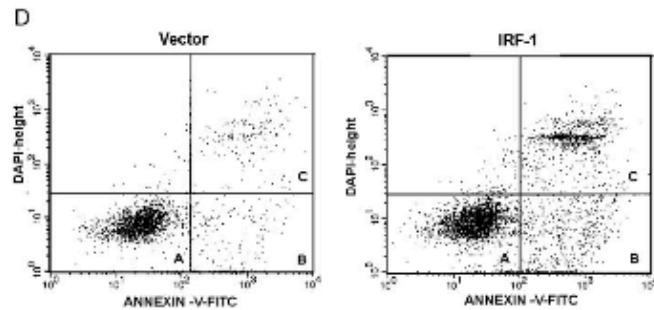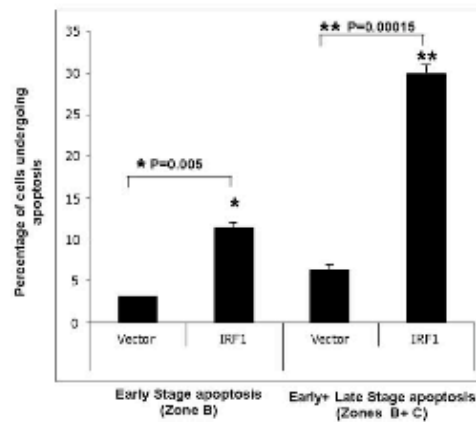
D

Fig. 2—*continued*

In order to determine whether activation of the NFκB signaling cascade by MIS was responsible for the induction of IRF-1 mRNA, we generated T47D cell clones which express the dominant negative inhibitor of IκB (IκBα-DN). In the rat IκBα-DN transgene used in these experiments, two serine residues at positions 32 and 36 are replaced by alanines. Hence the resulting IκBα-DN protein cannot be phosphorylated in response to activation signals. Thus it functions as a super repressor of NFκB activation (31). Two T47D cell clones expressing the IκBα-DN transgene were identified by the lack of NFκB activation following MIS treatment (Fig. 3D, *upper panel*). Induction of IRF-1 by MIS was greatly reduced in the two clones harboring IκBα-DN compared with cells transfected with the empty vector (Fig. 3D, *lower panel*). Thus MIS-induced IRF-1 requires activation of NFκB DNA binding activity. We next tested whether co-stimulation of IRF-1 by MIS and IFN-γ would be impaired in cells expressing IκBα-DN. Northern blot analysis of IκBα-DN-expressing cells treated with MIS, IFN-γ or both demonstrated that expression of IκBα-DN did not interfere with IFN-γ-induced IRF-1 expression. The stimulation of IRF-1 mRNA by a combination of MIS and IFN-γ was equivalent to that induced by IFN-γ alone since IRF-1 induction by MIS was impaired in these cells (Fig. 3E). Thus it is likely that co-stimulation of IRF-1 by MIS and IFN-γ in breast cancer cells is mediated through activation of NFκB and STAT pathways, respectively. Co-stimulation of IRF-1 was also observed when breast cancer cells were treated with a combination of MIS and IFN-β, a class I interferon (Fig. 3F).

Synergistic Induction of CEACAM1 by MIS and IFN-γ Is Mediated by IRF-1—CEACAM1 also known as biliary glycoprotein (BGP) is a Ca^{2+}-dependent cellular adhesion molecule that is expressed in epithelial cells (32, 33). An interferon-sensitive response element (ISRE) in the *CEACAM1* promoter is specifically protected by IRF-1 in DNA footprints and is required for induction of a *CEACAM1* promoter-driven reporter construct by IRF-1 (34). Both MIS and IFN-γ induced CEACAM1 expression in T47D cells (Fig. 4A, *left panel*). Induction of CEACAM1 by these two ligands was also observed in MDA-MD-468 cells (data not shown). Interestingly, simultaneous addition of MIS and IFN-γ resulted in synergistic induction of CEACAM1 expression (Fig. 4A, *right panel*).

In order to determine whether induction of CEACAM1 by MIS and IFN-γ was mediated through IRF-1, we generated T47D cells that stably express the antisense IRF-1 transcript. The ability of antisense IRF-1 to block the translation of IRF-1 protein was demonstrated by transient transfection of sense and antisense IRF-1 constructs into COS cells (Fig. 4B). Antisense IRF-1 expression inhibited the translation of IRF-1 protein derived from an IRF-1 expression construct. Phosphorimager analysis of CEACAM1 mRNA induction in breast cancer cells expressing antisense IRF-1 (Fig. 4C, *upper panel*) demonstrated that MIS- and IFN-γ-induced CEACAM1 expression by

28

FIG. 4. **Synergistic induction of CEACAM1 by MIS and IFN-γ is mediated by IRF-1.** *A, left panel,* T47D cells were treated with 35 nM MIS or 1 ng/ml of IFN-γ for increasing periods of time. Total RNA isolated from cells was analyzed for CEACAM1 expression by Northern blot. Hybridization to 18 S rRNA is shown. *Right panel,* T47D cells were treated with 35 nM MIS or 1 ng/ml of IFN-γ or both for 24 h. Total RNA isolated from cells was analyzed for CEACAM1 expression. Hybridization to 18 S rRNA is shown. *B,* antisense IRF-1 ablates translation of the IRF-1 protein. Lysates from COS cells transiently transfected with 1 μg of CMV-driven sense (*IRF-1-S*) or 2.9 μg of antisense IRF-1 (*IRF-IAS*) constructs or 2.9 μg of antisense + 1.0 μg of sense IRF-1 constructs were immunoblotted with an antibody to IRF-1. Position of the IRF-1 protein is indicated. *C,* synergistic induction of CEACAM1 by MIS and IFN-γ is impaired in T47D cells expressing antisense IRF-1. *Upper panel,* Northern blot analysis of total RNA isolated from T47D cells stably transfected with antisense IRF-1 demonstrates the expression of antisense IRF-1 transcript. *Lower panel,* cells were induced with 35 nM MIS or 1 ng/ml of IFN-γ or both for 24 h. Total RNA was analyzed by Northern blot for CEACAM1 expression. Fold change in CEACAM1 expression quantified using phosphorimager and iQMac data analysis software is shown below.
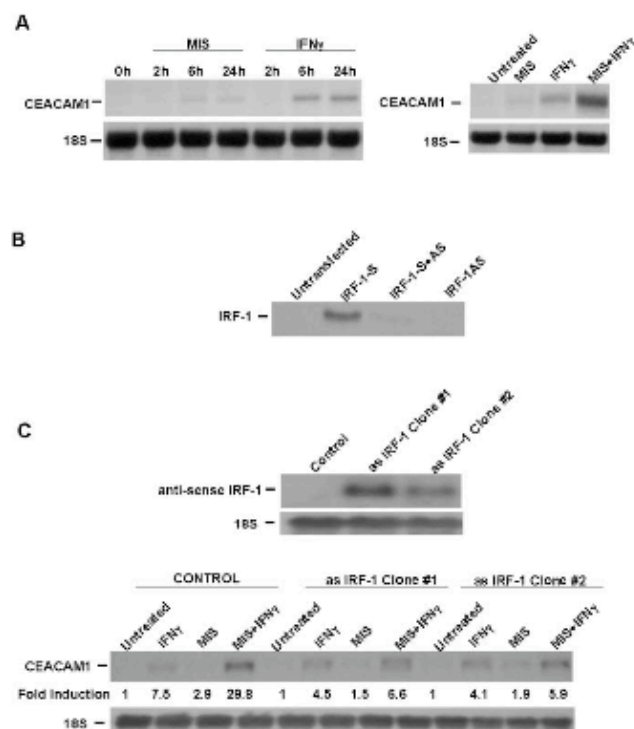
3- and 8-fold, respectively, in control cells and by 2- and 5-fold, respectively, in two clones expressing the antisense IRF-1 transcript suggesting that antisense IRF-1 slightly lowered CEACAM1 induction by MIS or IFN-γ (Fig. 4C, *lower panels*). However, the synergistic up-regulation of CECAM1 mRNA by combined treatment with MIS and IFN-γ was greatly impaired by the expression of antisense IRF-1; MIS and IFN-γ together induced CEACAM1 expression by 30-fold in control cells while its induction was additive (6–7-fold) in both clones expressing antisense-IRF-1 RNA (Fig. 4C, *lower panel*).

*Effect of MIS and IFN-γ on Breast Cancer Cell Growth—*Since the signaling events initiated by MIS and IFN-γ converge to increase the magnitude of gene expression, we next tested their effect on the growth of breast cancer cells. Treatment of MDA-MB-468 cells with either MIS or IFN-γ inhibited growth and the presence of both inhibited growth better (Fig. 5A; n = 8).

In order to identify the mechanism by which MIS and IFN-γ inhibit growth, assays to estimate cell cycle progression and apoptosis were performed. MDA-MB-468 cells were treated with MIS, IFN-γ, or MIS+IFN-γ for 72 h, and the fraction of cells in each phase of the cell cycle was estimated by fluorescence-activated cell sorting (Fig. 5B). Compared with untreated cells, MIS or IFN-γ treatment consistently led to a statistically significant decrease in the number of cells in the S-phase of the cell cycle (p < 0.001 by Student's t test). Interestingly, in cultures treated with a combination of MIS and IFN-γ, the percentage of cells in the S-phase did not demonstrate a greater decrease compared with that seen with either agent alone and these cultures did not exhibit any other extensive alteration in cell cycle distribution compared with cells treated with either agent alone. Thus the enhanced inhibition of breast cancer cell growth by MIS and IFN-γ could not be explained by combined changes in cell cycle progression compared with treatment with either agent alone.

Translocation of annexin V from the inner surface of the plasma membrane to the outside occurs after initiation of apoptosis and thus serves as a marker of apoptosis. MDA-MB-468 cells were treated with MIS, IFN-γ, or MIS+IFN-γ for 96 h and cell surface expression of annexin V was analyzed by staining with a FITC-annexin V antibody. Quantification of annexin V-positive cells demonstrated that IFN-γ is a strong inducer of

by Western blot. *Upper panel,* Immunoblot analysis with an antiphospho-STAT1 antibody. *Lower panel,* the blot was stripped and reanalyzed with an anti-STAT1 antibody. Positions of STAT1α and STAT1β are indicated. IFN-γ specifically induced the phosphorylation of STAT1α. *D,* MIS induces IRF-1 through activation of NFκB. T47D cells stably transfected with either vector or IκBα-DN were treated with MIS for 0 and 2 h. *Upper panel,* nuclear proteins were analyzed by gel-shift assay to determine NFκB DNA binding activity. Positions of the NFκB, DNA protein complexes are indicated. *Lower panel,* total cellular RNA (7.5 μg) was analyzed for induction of IRF-1. Hybridization to 18 S rRNA is shown as control for loading. *E,* vector and IκBα-DN-expressing T47D cells were treated with 35 nM MIS or 1 ng/ml of IFN-γ or both for 2 h, and total RNA (5 μg) was analyzed for IRF-1 expression. *F,* MIS and IFN-β co-stimulate IRF-1 expression. T47D cells were treated with 1 ng/ml of IFN-β or 17.5 nM MIS or a combination of 17.5 nM MIS and 1 ng/ml of IFN-β for 2 h. Total RNA isolated from cells was analyzed by Northern blot.

apoptosis in breast cancer cells (Fig. 5C). MIS consistently increased apoptosis in several experiments but its effect was much less potent than that of IFN-γ at the concentration tested. However, treatment of cells with a combination of MIS+IFN-γ together resulted in a synergistic increase in the fraction of cells in early and late stages of apoptosis. Thus growth inhibition of MDA-MB-468 cells following co-treatment with MIS and IFN-γ results from enhanced apoptosis rather than a combinatorial effect on the cell cycle.

DISCUSSION

MIS is a sexually dimorphic hormone that plays an important role in proper sexual development in male embryos (1). Interferons are antiviral and immunoregulatory proteins, which can negatively regulate growth in various cell types (35). IRF-1 mediates many IFN-γ-induced responses within cells by enhancing gene expression (14, 15) and its expression is also modulated by the cytokines TNF-α, IL-1, IL-6, and prolactin (15). TGFβ can either up- or down-regulate the expression of IRF-1 depending on its growth regulatory role in a particular cell type. In human embryonic lung fibroblasts, TGFβ-stimulated DNA synthesis was associated with suppression of IRF-1 expression whereas in human cholangiocarcinoma cells, TGFβ suppressed DNA synthesis through up-regulation of IRF-1 (36). Our results demonstrate that in addition to TGFβ, MIS and activin A also induce IRF-1 suggesting that members of the TGFβ superfamily may represent another class of molecules that can regulate IRF-1 expression.

Analysis of IRF-1 expression in the rat mammary gland demonstrated a gradual decline in mRNA that begins at the early stages of pregnancy suggesting that it may be a negative regulator of growth and/or differentiation in mammary epithelial cells. The RNA and protein were almost undetectable during late stages of pregnancy and lactation but recovered to levels seen in virgin animals nearly 3 days after removal of pups. However, Chapman et al. (37) analyzing total protein isolated from mammary glands of lactating and weaned mice by Western blot demonstrated that IRF-1 protein was expressed in the lactating mammary glands of mice and that levels did not change significantly during 24, 48, 72, and 96 h of involution. Western blot analysis is a more sensitive analytical tool than immunostaining to detect low levels protein expression. Thus it is possible that the discrepancy between these two observations results from the difference in sensitivity between the two techniques. Alternatively, the difference could also be attributed to the samples analyzed; total IRF-1 expression in the mammary gland (37) *versus* expression in the epithelial compartment in which IRF-1 protein expression is maintained at very low levels during late pregnancy, lactation, and early stages of involution but is up-regulated at weaning.

Many lines of evidence demonstrate that IRF1 plays a key role in growth control (25). The *IRF-1* gene maps to the chromosomal region 5q31.1 that is frequently deleted in human leukemia (38). The tumor suppressor activity of IRF-1 is also suggested by loss of an *IRF-1* allele in esophageal and gastric cancer (39–41). IRF-1 immunostaining of breast cancer specimens demonstrated that the protein was not detectable in 14% of invasive tumors. Expression did not correlate with estrogen receptor status or Page grade but correlated with nuclear

grade; it was undetectable in 41% of breast tumors of high nuclear grade (42). Consistent with the results reported by Doherty *et al.* (42), our results demonstrated loss of IRF-1 expression in 13% (3/23) of breast tumors compared with matched normal control tissue. Furthermore, 7 tumors demonstrated patchy staining in 20–80% of the tumor tissue. Thus some breast cancers may by-pass the growth-inhibitory effect exerted by IRF-1 by down-regulating its expression. In agreement with this concept, expression of IRF-1 in breast cancer cells results in the robust induction of apoptosis.

Paradoxically, examination of involuting mammary glands of IRF-1-null mice demonstrated accelerated apoptosis compared with wild-type mice at 48 h of involution. However, no difference in morphology was evident in the mammary glands isolated from control and IRF-1-null mice at 72 h of involution (37). These results suggest that IRF-1 may be a suppressor of premature epithelial apoptosis in the mammary gland. Thus it is possible that IRF-1 serves different functions during various stages of postnatal mammary gland development, neoplastic transformation, and tumorigenic process of the breast.

Induction of IRF-1 by IFN-γ occurs through phosphorylation of the latent transcription factor STAT1, homodimers of which bind to the *IRF-1* promoter (15). However, the presence of a putative NFκB site within the *IRF-1* promoter (43, 44) renders it responsive to extracellular signals that activate the NFκB pathway. Induction of IRF-1 by MIS in breast cancer cells was mediated by activation of NFκB and addition of methylthioadenosine to inhibit STAT1 methylation (45) lowered IFN-γ-induced IRF-1 expression (data not shown). Thus IRF-1 co-stimulation by MIS and IFN-γ in breast cancer cells may occur through activation of these two pathways.

Several growth regulatory genes including those with antiproliferative activity such as IFNα/β, p21, and CEACAM1 have IRF-1 DNA recognition sites in their promoters (25, 34). In HeLa and HT-29 cells, IFN-γ up-regulated a *CEACAM1* promoter-driven-luciferase construct by 2- and 2.5-fold, respectively, an effect that was abrogated upon mutating the interferon response element that binds IRF-1 (34). However, this report did not evaluate the effect of IFN-γ and IFN-γ-induced IRF-1 on the induction of endogenous CEACAM1 mRNA. In breast cancer cells expression of antisense IRF-1, which ablates translation of the IRF-1 protein decreased CEACAM1 induction slightly when MIS and IFN-γ were used alone suggesting that IRF-1 may be partially responsible for this inductive process. Quantification of band intensities demonstrated that induction of CEACAM1 by a combination of MIS and IFN-γ was strictly additive in T47D cells expressing antisense IRF-1. However, the synergistic up-regulation of CEACAM1 by MIS and IFN-γ was completely abrogated in both T47D cell clones stably expressing the antisense IRF-1 transcript suggesting that IRF-1 may be involved in the interaction between MIS and IFN-γ leading to the synergistic induction of CEACAM1.

IRF-1 has been implicated in mediating the IFN-γ contribution to synergistic enhancement of transcription in other experimental systems. Enhancer elements that bind IFN-γ-responsive transcription factors including an IRF-1 binding site have been shown to be involved in the synergistic induction of the *iNOS* promoter-driven luciferase construct by IFN-γ (46).

---

incubated with propidium iodide and RNase A. DNA content was analyzed by FACS. Cell cycle analysis of untreated cells grown for 72 h is shown as control. Statistical analysis was done using Student's *t* test. *C,* MIS promotes IFN-γ-induced apoptosis. MDA-MB-468 cells were treated with MIS and IFN-γ at a concentration of 35 nM and 5 ng/ml, respectively for 96 h. Cells were stained with annexin V-FITC, and DAPI and analyzed by FACS. *Upper panels,* representative experiments demonstrating DAPI ± and annexin V ± cells are shown. Zones A (DAPI-negative, annexin V-negative) and B (DAPI-negative, annexin V-positive) represent live and early apoptotic cells, respectively. Zone C represents cells in late stage apoptosis (DAPI-positive, annexin V-positive). *Lower panel* shows the percentage of cells in early (*Zone B*) and early + late stages (*Zones B+C*) of apoptosis (*n* = 3). Statistical analysis was done using Student's *t* test.

In IRF-1-null macrophages, the ability of IFN-γ to up-regulate as well as synergistically induce Cox-2 mRNA expression was abrogated (47). The synergistic induction of transcription by IRF-1 has been shown to depend on protein-protein interaction (48–50). Further analysis of the *CEACAM1* promoter-driven reporter construct may be required to delineate the process by which IRF-1 mediates the synergistic interaction between MIS and IFN-γ in the induction of the *CEACAM1* gene in breast cancer cells.

CEACAM1, located on chromosome 19 (51), is down-regulated in human colon and prostate cancers (52, 53) and in about 30% of breast carcinomas (54, 55). Consistent with its tumor suppressor function, introduction of CEACAM1 into MDA-MB-468 cells suppressed tumorigenicity in nude mice (56). In normal mammary epithelial cells, CEACAM1 staining is confined to the luminal surface and its localized expression appears to be important in lumen formation (55, 57) suggesting that CEACAM1 expression may be important in differentiation of mammary epithelial cells. Furthermore, expression of CEACAM1 in the BGP-negative MCF7 cells induces cell death with occasional formation of acini when grown in extracellular matrix (57). The synergistic up-regulation of CEACAM1 by MIS and IFN-γ suggests that the level of CEACAM1 expression in the mammary epithelial cells may depend on the integrated response to various extracellular signals received by the cell. Whether the synergistic induction of CEACAM1 by MIS and IFN-γ can reinitiate the differentiation program in breast cancer cells remains to be determined.

IFN-γ in combination with IFN-β has been shown to induce the regression of human breast cancer cell lines MCF7 and BT20 grown as xenografts in nude mice (58). Although the antitumor effect of IFN-γ *in vivo* has been well documented, toxicity associated with exposure to IFN-γ has diminished its utility in treatment (59). The ability of MIS to augment IFN-γ-induced growth inhibitory/differentiation signals such as CEACAM1 and apoptosis of breast cancer cell growth, suggests that MIS may prove to be beneficial in harnessing the antitumor effects of this cytokine, especially since high levels of MIS have not shown any harmful effects in humans (60).

REFERENCES

1. Teixeira, J., Maheswaran, S., and Donahoe, P. K. (2001) *Endocrinol. Rev.* **22**, 657–674
2. Hoshiya, Y., Gupta, V., Segev, D. L., Hoshiya, M., Carey, J. L., Sasur, L. M., Tran, T. T., Ha, T. U., and Maheswaran, S. (2003) *Mol. Cell. Endocrinol.*
3. Segev, D. L., Hoshiya, Y., Stephen, A. E., Hoshiya, M., Tran, T. T., MacLaughlin, D. T., Donahoe, P. K., and Maheswaran, S. (2001) *J. Biol. Chem.* **276**, 26799–26806
4. Segev, D. L., Ha, T. U., Tran, T. T., Kenneally, M., Harkin, P., Jung, M., MacLaughlin, D. T., Donahoe, P. K., and Maheswaran, S. (2000) *J. Biol. Chem.* **275**, 28371–28379
5. Stark, G. R., Kerr, I. M., Williams, B. R., Silverman, R. H., and Schreiber, R. D. (1998) *Annu. Rev. Biochem.* **67**, 227–264
6. Gollob, J. A., Mier, J. W., Veenstra, K., McDermott, D. F., Clancy, D., Clancy, M., and Atkins, M. B. (2000) *Clin. Cancer Res.* **6**, 1678–1692
7. Brunda, M. J., Luistro, L., Hendrzak, J. A., Fountoulakis, M., Garotta, G., and Gately, M. K. (1995) *J. Immunother. Emphasis Tumor Immunol.* **17**, 71–77
8. Brunda, M. J., Luistro, L., Rumennik, L., Wright, R. B., Wigginton, J. M., Wiltrout, R. H., Hendrzak, J. A., and Palleroni, A. V. (1996) *Ann. N. Y. Acad. Sci.* **795**, 266–274
9. Brunda, M. J., Luistro, L., Rumennik, L., Wright, R. B., Dvorozniak, M., Aglione, A., Wigginton, J. M., Wiltrout, R. H., Hendrzak, J. A., and Palleroni, A. V. (1996) *Cancer Chemother. Pharmacol.* **38**, (suppl.) S16–S21
10. Cifaldi, L., Quaglino, E., Di Carlo, E., Musiani, P., Spadaro, M., Lollini, P. L., Wolf, S., Boggio, K., Forni, G., and Cavallo, F. (2001) *Cancer Res.* **61**, 2809–2812
11. Wigginton, J. M., Park, J. W., Gruys, M. E., Young, H. A., Jorcyk, C. L., Back, T. C., Brunda, M. J., Strieter, R. M., Ward, J., Green, J. E., and Wiltrout, R. H. (2001) *J. Immunol.* **166**, 1156–1168
12. Wigginton, J. M., Gruys, E., Geiselhart, L., Subleski, J., Komschlies, K. L., Park, J. W., Wiltrout, T. A., Nagashima, K., Back, T. C., and Wiltrout, R. H. (2001) *J. Clin. Invest.* **108**, 51–62
13. Kalvakolanu, D. V. (2000) *Histol. Histopathol.* **15**, 523–537
14. Taniguchi, T., Lamphier, M. S., and Tanaka, N. (1997) *Biochim. Biophys. Acta* **1333**, M9–17
15. Taniguchi, T., Ogasawara, K., Takaoka, A., and Tanaka, N. (2001) *Annu. Rev. Immunol.* **19**, 623–655
16. Taniguchi, T., and Takaoka, A. (2002) *Curr. Opin. Immunol.* **14**, 111–116
17. Haus, O. (2000) *Arch. Immunol. Ther. Exp. (Warsz)* **48**, 95–100
18. Wadler, S., and Schwartz, E. L. (1990) *Cancer Res.* **50**, 3473–3486
19. Strander, H. (1986) *Adv. Cancer Res.* **46**, 1–265
20. Kirchhoff, S., and Hauser, H. (1999) *Oncogene* **18**, 3725–3736
21. Ruiz-Ruiz, C., Munoz-Pinedo, C., and Lopez-Rivas, A. (2000) *Cancer Res.* **60**, 5673–5680
22. Hadden, J. W. (1999) *Int. J. Immunopharmacol.* **21**, 79–101
23. Habif, D. V., Ozzello, L., De Rosa, C. M., Cantell, K., and Lattes, R. (1995) *Cancer Invest.* **13**, 165–172
24. Ogasawara, K., Hida, S., Azimi, N., Tagaya, Y., Sato, T., Yokochi-Fukuda, T., Waldmann, T. A., Taniguchi, T., and Taki, S. (1998) *Nature* **391**, 700–703
25. Romeo, G., Fiorucci, G., Chiantore, M. V., Percario, Z. A., Vannucchi, S., and Affabris, E. (2002) *J. Interferon. Cytokine Res.* **22**, 39–47
26. Ragin, R. C., Donahoe, P. K., Kenneally, M. K., Ahmad, M. F., and MacLaughlin, D. T. (1992) *Protein Expr. Purif.* **3**, 236–245
27. Ha, T. U., Segev, D. L., Barbie, D., Masiakos, P. T., Tran, T. T., Dombkowski, D., Glander, M., Clarke, T. R., Lorenzo, H. K., Donahoe, P. K., and Maheswaran, S. (2000) *J. Biol. Chem.* **275**, 37101–37109
28. van den Heuvel, S., and Harlow, E. (1993) *Science* **262**, 2050–2054
29. Kurian, M. S., de la Cuesta, R. S., Waneck, G. L., MacLaughlin, D. T., Manganaro, T. F., and Donahoe, P. K. (1995) *Clin. Cancer Res.* **1**, 343–349
30. Seuls, H. D., Maloney, T. M., Wolman, S. R., Peterson, W. D., Brenz, R., McGrath, C. M., Russo, J., Pauley, R. J., Jones, R. F., and Brooks, S. C. (1990) *Cancer Res.* **50**, 6075–6086
31. Brown, K., Gerstberger, S., Carlson, L., Franzoso, G., and Siebenlist, U. (1995) *Science* **267**, 1485–1488
32. Thompson, N. L., Lin, S. H., Panzica, M. A., and Hixson, D. C. (1994) *Pathobiology* **62**, 209–220
33. Cheung, P. H., Thompson, N. L., Earley, K., Culic, O., Hixson, D., and Lin, S. H. (1993) *J. Biol. Chem.* **268**, 6139–6146
34. Chen, C. J., Lin, T. T., and Shively, J. E. (1996) *J. Biol. Chem.* **271**, 28181–28188
35. Tanaka, N., and Taniguchi, T. (2000) *Semin. Cancer Biol.* **10**, 73–81
36. Miyazaki, M., Ohashi, R., Tsuji, T., Mihara, K., Gohda, E., and Namba, M. (1998) *Biochem. Biophys. Res. Commun.* **246**, 873–880
37. Chapman, R. S., Duff, E. K., Lourenco, P. C., Tonner, E., Flint, D. J., Clarke, A. R., and Watson, C. J. (2000) *Oncogene* **19**, 6386–6391
38. Willman, C. L., Sever, C. E., Pallavicini, M. G., Harada, H., Tanaka, N., Slovak, M. L., Yamamoto, H., Harada, K., Meeker, T. C., List, A. F., and Taniguchi, T. (1993) *Science* **259**, 968–971
39. Ogasawara, S., Tamura, G., Maesawa, C., Suzuki, Y., Ishida, K., Satoh, N., Uesugi, N., Saito, K., and Satodate, R. (1996) *Gastroenterology* **110**, 52–57
40. Nozawa, H., Oda, E., Ueda, S., Tamura, G., Maesawa, C., Muto, T., Taniguchi, T., and Tanaka, N. (1998) *Int. J. Cancer* **77**, 522–527
41. Tamura, G., Ogasawara, S., Nishizuka, S., Sakata, K., Maesawa, C., Suzuki, Y., Terashima, M., Saito, K., and Satodate, R. (1995) *Cancer Res.* **56**, 612–615
42. Doherty, G. M., Boucher, L., Sorenson, K., and Lowney, J. (2001) *Ann. Surg.* **233**, 623–629
43. Sims, S. H., Cha, Y., Romine, M. F., Gao, P. Q., Gottlieb, K., and Deisseroth, A. B. (1993) *Mol. Cell. Biol.* **13**, 690–702
44. Ohmori, Y., Schreiber, R. D., and Hamilton, T. A. (1997) *J. Biol. Chem.* **272**, 14899–14907
45. Zhu, W., Mustelin, T., and David, M. (2002) *J. Biol. Chem.* **277**, 35787–35790
46. Martin, E., Nathan, C., and Xie, Q. W. (1994) *J. Exp. Med.* **180**, 977–984
47. Blanco, J. C., Contursi, C., Salkowski, C. A., DeWitt, D. L., Ozato, K., and Vogel, S. N. (2000) *J. Exp. Med.* **191**, 2131–2144
48. Eklund, E. A., Jalava, A., and Kakar, R. (1998) *J. Biol. Chem.* **273**, 13957–13965
49. Marecki, S., Riendeau, C. J., Liang, M. D., and Fenton, M. J. (2001) *J. Immunol.* **166**, 6829–6838
50. Tendler, D. S., Bao, C., Wang, T., Huang, E. L., Ratovitski, E. A., Pardoll, D. A., and Lowenstein, C. J. (2001) *Cancer Res.* **61**, 3682–3688
51. Thompson, J., Zimmermann, W., Osthus-Bugat, P., Schleussner, C., Eades-Perner, A. M., Barnert, S., Von Kleist, S., Willcocks, T., Craig, I., Tynan, K., Olsen, A., and Mohrenweiser, H. (1992) *Genomics* **12**, 761–772
52. Hsieh, J. T., Luo, W., Song, W., Wang, Y., Kleinerman, D. I., Van, N. T., and Lin, S. H. (1995) *Cancer Res.* **55**, 190–197
53. Luo, W., Tapolsky, M., Earley, K., Wood, C. G., Wilson, D. R., Logothetis, C. J., and Lin, S. H. (1999) *Cancer Gene Ther.* **6**, 313–321
54. Riethdorf, L., Lisboa, B. W., Henkel, U., Naumann, M., Wagener, C., and Loning, T. (1997) *J. Histochem. Cytochem.* **45**, 957–963
55. Huang, J., Simpson, J. F., Glackin, C., Riethorf, L., Wagener, C., and Shively, J. E. (1998) *Anticancer Res.* **18**, 3203–3212
56. Luo, W., Wood, C. G., Earley, K., Hung, M. C., and Lin, S. H. (1997) *Oncogene* **14**, 1697–1704
57. Huang, J., Hardy, J. D., Sun, Y., and Shively, J. E. (1999) *J. Cell Sci.* **112**, 4193–4205
58. Ozzello, L., Habif, D. V., and DeRosa, C. M. (1990) *Breast Cancer Res. Treat* **16**, 89–96
59. Borden, E. C., Lindner, D., Dreicer, R., Hussein, M., and Peereboom, D. (2000) *Semin. Cancer Biol.* **10**, 125–144
60. Gustafson, M. L., Lee, M. M., Scully, R. E., Moncure, A. C., Hirakawa, T., Goodman, A., Muntz, H. G., Donahoe, P. K., MacLaughlin, D. T., and Fuller, A. F., Jr. (1992) *N. Engl. J. Med.* **326**, 466–471